EUROPEAN ORGANIZATION FOR NUCLEAR RESEARCH (CERN)

CERN-EP-2019-029
2019/03/19

CMS-HIG-17-034

Constraints on anomalous HVV couplings from the production of Higgs bosons decaying to τ lepton pairs

The CMS Collaboration*

Abstract

A study is presented of anomalous HVV interactions of the Higgs boson, including its CP properties. The study uses Higgs boson candidates produced mainly in vector boson fusion and gluon fusion that subsequently decay to a pair of τ leptons. The data were recorded by the CMS experiment at the LHC in 2016 at a center-of-mass energy of 13 TeV and correspond to an integrated luminosity of 35.9 fb^{-1}. A matrix element technique is employed for the analysis of anomalous interactions. The results are combined with those from the $\text{H} \to 4\ell$ decay channel presented earlier, yielding the most stringent constraints on anomalous Higgs boson couplings to electroweak vector bosons expressed as effective cross-section fractions and phases: the CP-violating parameter $f_{a3}\cos(\phi_{a3}) = (0.00 \pm 0.27) \times 10^{-3}$ and the CP-conserving parameters $f_{a2}\cos(\phi_{a2}) = (0.08^{+1.04}_{-0.21}) \times 10^{-3}$, $f_{\Lambda 1}\cos(\phi_{\Lambda 1}) = (0.00^{+0.53}_{-0.09}) \times 10^{-3}$, and $f_{\Lambda 1}^{\text{Z}\gamma}\cos(\phi_{\Lambda 1}^{\text{Z}\gamma}) = (0.0^{+1.1}_{-1.3}) \times 10^{-3}$. The current data set does not allow for precise constraints on CP properties in the gluon fusion process. The results are consistent with standard model expectations.

Submitted to Physical Review D

*See Appendix A for the list of collaboration members

1 Introduction

The Higgs boson (H) discovered in 2012 at the CERN LHC [1–3] has thus far been found to have properties consistent with expectations from the standard model (SM) [4–10]. In particular, its spin-parity quantum numbers are consistent with $J^{PC} = 0^{++}$ according to measurements performed by the CMS [11–17] and ATLAS [18–23] experiments. It is still to be determined whether small anomalous couplings contribute to the HVV or Hff interactions, where V stands for vector bosons and f for fermions. Because nonzero spin assignments of the H boson have been excluded [13, 19], we focus on the analysis of couplings of a spin-zero H boson. Previous studies of anomalous HVV couplings were performed by both the CMS and ATLAS experiments using either decay-only information [11–13, 18, 19, 21], including associated production information [15–17, 20, 22, 23], or including off-shell H boson production [14, 17]. In this paper, we report a study of HVV couplings using information from production of the H boson decaying to τ leptons. These results are combined with the previous CMS measurements using both associated production and decay information in the $\mathrm{H} \to 4\ell$ channel [17], resulting in stringent constraints on anomalous H boson couplings. Here and in the following ℓ denotes an electron or muon.

The $\mathrm{H} \to \tau\tau$ decay has been observed by the CMS experiment, with over five standard deviation significance [24]. The $\mathrm{H} \to \tau\tau$ sample can be used to study the quantum numbers of the H boson and its anomalous couplings to SM particles, including its CP properties. The dominant production mechanisms of the H boson considered in this paper are shown at leading order in QCD in Fig. 1. The correlations between the H boson, the beamline, and the two jets in vector boson fusion (VBF), associated production with a vector boson decaying hadronically (VH, where $\mathrm{V} = \mathrm{W}, \mathrm{Z}$), or gluon fusion production with an additional two jets are sensitive to anomalous HWW, HZZ, HZγ, H$\gamma\gamma$, and Hgg couplings, which are the focus of this paper. The gluon fusion production with an additional two jets appears at higher order in QCD with an example of gluons appearing in place of the vector bosons shown in the VBF diagram in the middle of Fig. 1. A study of anomalous H$\mathrm{t\bar{t}}$ couplings in associated production with top quarks, $\mathrm{t\bar{t}H}$ or tqH, and anomalous H$\tau\tau$ couplings in the decay of the H boson are also possible using $\tau\tau$ events [25]. However, more data are needed to reach sensitivity to such anomalous effects, and it has been confirmed that these anomalous couplings would not affect the measurements presented in this paper.

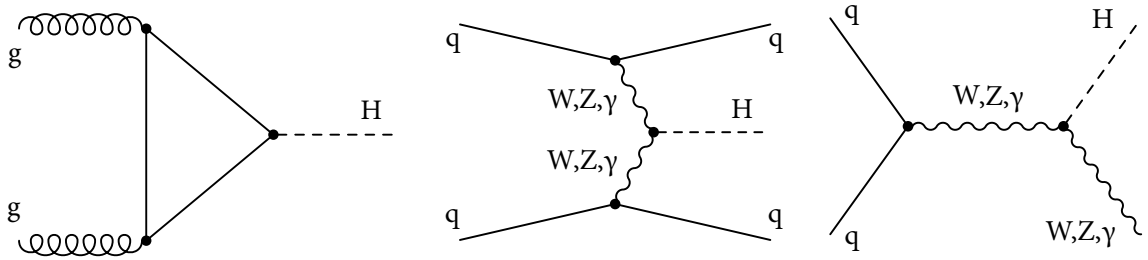

Figure 1: Examples of leading-order Feynman diagrams for H boson production via the gluon fusion (left), vector boson fusion (middle), and associated production with a vector boson (right). The HWW and HZZ couplings may appear at tree level, as the SM predicts. Additionally, HWW, HZZ, HZγ, H$\gamma\gamma$, and Hgg couplings may be generated by loops of SM or unknown particles, as indicated in the left diagram but not shown explicitly in the middle and right diagrams.

To increase the sensitivity to anomalous couplings in the H boson production, the matrix element likelihood approach (MELA) [2, 26–29] is utilized to form optimal observables. The analysis is optimized for VBF production and is not additionally optimized for VH or gluon fusion

production. However, all three production mechanisms are included in the analysis, using a general anomalous coupling parameterization. The $H \to \tau\tau$ channel has advantages over other H boson decay channels because of the relatively high significance of the signal events in the VBF channel [24]. Three mutually exclusive categories of events are reconstructed in the analysis: the VBF category targets events with two associated jets in the VBF event topology, the boosted category contains events with one jet or more jets if the event is not in the VBF category, and the 0-jet category targets H boson events produced via gluon fusion without associated jets. The simultaneous analysis of all three categories of events is necessary to boost the sensitivity to anomalous HVV couplings from events with partial kinematic information reconstructed in the non-VBF categories and to normalize the relative contribution of different production mechanisms.

The analysis utilizes the same data as Ref. [24] and follows closely the event selection and categorization described in Section 3. The phenomenological model and Monte Carlo (MC) simulation are described in Section 4. The matrix element techniques used to extract the kinematic information are discussed in Section 5. The implementation of the likelihood fit using kinematic information in the events is presented in Section 6. The results are presented and discussed in Sections 7 and 8, before conclusions are drawn in Section 9.

2 The CMS detector

The central feature of the CMS apparatus is a superconducting solenoid of 6 m internal diameter, providing a magnetic field of 3.8 T. Within the solenoid volume, there are a silicon pixel and strip tracker, a lead tungstate crystal electromagnetic calorimeter (ECAL), and a brass and scintillator hadron calorimeter, each composed of a barrel and two endcap sections. Forward calorimeters extend the pseudorapidity, η, coverage provided by the barrel and endcap detectors. Muons are detected in gas-ionization chambers embedded in the steel flux-return yoke outside the solenoid.

Events of interest are selected using a two-tiered trigger system [30]. The first level (L1), composed of custom hardware processors, uses information from the calorimeters and muon detectors to select events at a rate of around 100 kHz within a time interval of less than 4 μs. The second level, known as the high-level trigger, consists of a farm of processors running a version of the full event reconstruction software optimized for fast processing, and reduces the event rate to about 1 kHz before data storage.

A more detailed description of the CMS detector, together with a definition of the coordinate system used and the relevant kinematic variables, can be found in Ref. [31].

The data samples used in this analysis correspond to an integrated luminosity of 35.9 fb^{-1} collected in Run 2 of the LHC during 2016 at a center-of-mass energy of 13 TeV.

3 Event reconstruction and selection

The analysis uses the same data set, event reconstruction, and selection criteria as those used in the analysis leading to the observation of the H boson decay to a pair of τ leptons [24].

3.1 Event reconstruction

The reconstruction of observed and simulated events relies on the particle-flow (PF) algorithm [32], which combines the information from the CMS subdetectors to identify and re-

construct particles emerging from pp collisions. Combinations of these PF candidates are used to reconstruct higher-level objects such as jets, τ candidates, or missing transverse momentum, $\vec{p}_{\mathrm{T}}^{\,\mathrm{miss}}$. The reconstructed vertex with the largest value of summed physics-object p_{T}^2 is taken to be the primary pp interaction vertex, where p_{T} is the transverse momentum. The physics objects are the objects constructed by a jet finding algorithm [33, 34] applied to all charged tracks associated with the vertex, and the corresponding associated missing transverse momentum.

Electrons are identified with a multivariate discriminant combining several quantities describing the track quality, the shape of the energy deposits in the ECAL, and the compatibility of the measurements from the tracker and the ECAL [35]. Muons are identified with requirements on the quality of the track reconstruction and on the number of measurements in the tracker and the muon systems [36]. To reject nonprompt or misidentified leptons, an isolation requirement I^{ℓ} is applied according to the criteria described in Ref. [24].

Jets are reconstructed with an anti-k_{T} clustering algorithm [37], as implemented in the FastJet package [34]. It is based on the clustering of neutral and charged PF candidates within a distance parameter of 0.4. Charged PF candidates not associated with the primary vertex of the interaction are not considered when building jets. An offset correction is applied to jet energies to take into account the contribution from additional pp interactions within the same or nearby bunch crossings. In this analysis, jets are required to have $p_{\mathrm{T}} > 30\,\mathrm{GeV}$ and absolute pseudorapidity $|\eta| < 4.7$, and to be separated from the selected leptons by a distance parameter $\Delta R = \sqrt{(\Delta\eta)^2 + (\Delta\phi)^2}$ of at least 0.5, where ϕ is the azimuthal angle in radians. The combined secondary vertex algorithm is used to identify jets that are likely to originate from a bottom quark ("b jets"). The algorithm exploits track-based lifetime information along with the secondary vertex of the jet to provide a likelihood ratio discriminator for b jet identification.

Hadronically decaying τ leptons, denoted as τ_{h}, are reconstructed with the hadron-plus-strips algorithm [38, 39], which is seeded with anti-k_{T} jets. This algorithm reconstructs τ_{h} candidates based on the number of tracks and the number of ECAL strips with energy deposits within the associated η-ϕ plane, and reconstructs 1-prong, 1-prong+π^0(s), and 3-prong decay modes, identified as $M = 1, 2$, and 3, respectively. A multivariate (MVA) discriminator, including isolation and lifetime information, is used to reduce the rate for quark- and gluon-initiated jets to be identified as τ_{h} candidates. The working point used in this analysis has an efficiency of about 60% for genuine τ_{h}, with about 1% misidentification rate for quark- and gluon-initiated jets, for a p_{T} range typical of τ_{h} originating from a Z boson. Electrons and muons misidentified as τ_{h} candidates are suppressed using dedicated criteria based on the consistency between the measurements in the tracker, the calorimeters, and the muon detectors [38, 39]. The τ_{h} energy scale as well as the rate and the energy scale of electrons and muons misidentified as τ_{h} candidates are corrected in simulation to match those measured in data [24].

The missing transverse momentum is defined as the negative vector sum of the transverse momenta of all PF candidates [40]. The details of the corrections to $\vec{p}_{\mathrm{T}}^{\,\mathrm{miss}}$ for the mismodeling in the simulation of Z + jets, W + jets, and H boson processes are described in Ref. [24].

Both the visible mass of the $\tau\tau$ system m_{vis} and the invariant mass of the $\tau\tau$ system $m_{\tau\tau}$ are used in the analysis. The visible mass is defined as the invariant mass of the visible decay products of the τ leptons. The observable $m_{\tau\tau}$ is reconstructed using the SVFIT [41] algorithm, which combines the $\vec{p}_{\mathrm{T}}^{\,\mathrm{miss}}$ and its uncertainty with the four-vectors of both τ candidates to calculate a more accurate estimate of the mass of the parent boson. The estimate of the four-momentum of the H boson provided by SVFIT is used to calculate the kinematic observables discussed in Section 5.

3.2 Event selection and categorization

Selected events are classified according to four decay channels, $e\mu$, $e\tau_h$, $\mu\tau_h$, and $\tau_h\tau_h$. The resulting event samples are made mutually exclusive by discarding events that have additional loosely identified and isolated electrons or muons.

The largest irreducible source of background is Drell-Yan production of $Z \to \tau\tau$, while the dominant background sources with jets misidentified as leptons are QCD multijet and $W+$jets. Other contributing background sources are $t\bar{t}$, single top, $Z \to \ell\ell$ and diboson production.

The two leptons assigned to the H boson decay are required to have opposite charges. The trigger requirements, geometrical acceptances, and transverse momentum criteria are summarized in Table 1. The p_T thresholds in the lepton selections are optimized to increase the sensitivity to the $H \to \tau\tau$ signal, while also satisfying the trigger requirements.

Table 1: Kinematic selection criteria for the four decay channels. For the trigger threshold requirements, the numbers indicate the trigger thresholds in GeV. The lepton selection criteria include the transverse momentum threshold, pseudorapidity range, as well as isolation criteria.

Channel	Trigger requirement	Lepton selection	
	p_T (GeV)	p_T (GeV)	η
$e\mu$	$p_T^e > 12$ & $p_T^\mu > 23$	$p_T^e > 13$	$\lvert\eta^e\rvert < 2.5$
		$p_T^\mu > 24$	$\lvert\eta^\mu\rvert < 2.4$
	$p_T^e > 23$ & $p_T^\mu > 8$	$p_T^e > 24$	$\lvert\eta^e\rvert < 2.5$
		$p_T^\mu > 15$	$\lvert\eta^\mu\rvert < 2.4$
$e\tau_h$	$p_T^e > 25$	$p_T^e > 26$	$\lvert\eta^e\rvert < 2.1$
		$p_T^{\tau_h} > 30$	$\lvert\eta^{\tau_h}\rvert < 2.3$
$\mu\tau_h$	$p_T^\mu > 22$	$p_T^\mu > 23$	$\lvert\eta^\mu\rvert < 2.1$
		$p_T^{\tau_h} > 30$	$\lvert\eta^{\tau_h}\rvert < 2.3$
	$p_T^\mu > 19$ & $p_T^{\tau_h} > 21$	$20 < p_T^\mu < 23$	$\lvert\eta^\mu\rvert < 2.1$
		$p_T^{\tau_h} > 30$	$\lvert\eta^{\tau_h}\rvert < 2.3$
$\tau_h\tau_h$	$p_T^{\tau_h} > 35$ & 35	$p_T^{\tau_h} > 50$ & 40	$\lvert\eta^{\tau_h}\rvert < 2.1$

In the $\ell\tau_h$ channels, where $\ell = e, \mu$, the large $W+$jets background is reduced by requiring the transverse mass, m_T, to be less than 50 GeV. The transverse mass is defined as follows

$$m_T \equiv \sqrt{2 p_T^\ell p_T^{\text{miss}} [1 - \cos(\Delta\phi)]}, \tag{1}$$

where p_T^ℓ is the transverse momentum of the electron or muon, and $\Delta\phi$ is the azimuthal angle between that lepton and the $\vec{p}_T^{\,\text{miss}}$ directions.

In the $e\mu$ channel, the $t\bar{t}$ background is reduced by requiring $p_\zeta - 0.85\, p_\zeta^{\text{vis}} > -35$ GeV or -10 GeV depending on the category, where p_ζ is the component of $\vec{p}_T^{\,\text{miss}}$ along the bisector of the transverse momenta of the two leptons and p_ζ^{vis} is the sum of the components of the lepton transverse momenta along the same direction [42]. In addition, events with a b-tagged jet are discarded to further suppress the $t\bar{t}$ background in this channel.

In the same way as in Ref. [24], the event samples are split into three mutually exclusive production categories:

- 0-jet category: This category targets H boson events produced via gluon fusion. Events containing no jets with $p_T > 30\,\text{GeV}$ are selected. Simulations indicate that about 98% of signal events in the 0-jet category arise from the gluon fusion production mechanism.

- VBF category: This category targets H boson events produced via the VBF process. Events are selected with exactly (at least) two jets with $p_T > 30\,\text{GeV}$ in the eμ (eτ_h, $\mu\tau_h$, and $\tau_h\tau_h$) channels. In the $\mu\tau_h$, eτ_h, and eμ channels, the two leading jets are required to have an invariant mass, m_{JJ}, larger than 300 GeV. The vector sum of the $\vec{p}_T^{\,\text{miss}}$ and the p_T of the visible decay products of the tau leptons, defined as $p_T^{\tau\tau}$, is required to be greater than 50 (100) GeV in the $\ell\tau_h$ ($\tau_h\tau_h$) channels. In addition, the p_T threshold on the τ_h candidate is raised to 40 GeV in the $\mu\tau_h$ channel, and the two leading jets in the $\tau_h\tau_h$ channel must be separated in pseudorapidity by $|\Delta\eta| > 2.5$. Depending on the decay channel, up to 57% of the signal events in the VBF category are produced via VBF. This fraction increases with m_{JJ}. Gluon fusion production makes 40-50% of the total signal, while the VH contribution is less than 3%.

- Boosted category: This category contains all the events that do not enter one of the previous categories, namely events with one jet and events with several jets that fail the requirements of the VBF category. It targets events with a H boson produced in gluon fusion and recoiling against an initial state radiation jet. It contains gluon fusion events produced in association with one or more jets (78–80% of the signal events), VBF events in which one of the jets has escaped detection or events with low m_{JJ} (11–13%), as well as H boson events produced in association with a W or a Z boson decaying hadronically (4–8%).

In addition to these three signal regions for each channel, a series of control regions targeting different background processes are included in the maximum likelihood fit used to extract the results of the analysis. The normalization of the W + jets background in the eτ_h and $\mu\tau_h$ channels is estimated from simulations, and adjusted to data using control regions obtained by applying all selection criteria, with the exception that m_T is required to be greater than 80 GeV instead of less than 50 GeV. The normalization of the QCD multijet background in the eτ_h and $\mu\tau_h$ channels is estimated from events where the electron or the muon has the same charge as the τ_h candidate. The factor to extrapolate from the same-sign to the opposite-sign region is constrained by adding the opposite-sign region, where the ℓ candidates pass inverted isolation criteria to the global fit.

In the $\tau_h\tau_h$ channel, the QCD multijet background is estimated from events where the τ_h candidates pass relaxed isolation conditions, and the extrapolation factor is derived from events where the τ_h candidates have charges of the same sign. The events selected with opposite-sign τ_h candidates passing relaxed isolation requirements form a control region included in the global fit. Finally, the normalization of the $\mathrm{t\bar{t}}$ background is adjusted using a control region defined similarly as the eμ signal region, except that the p_ζ requirement is inverted and the events are required to contain at least one jet.

4 Phenomenology of anomalous couplings and simulation

We follow the formalism used in the study of anomalous couplings in earlier analyses by CMS [11–17]. The theoretical approach is described in Refs. [26–29, 43–51]. Anomalous interactions of a spin-zero H boson with two spin-one gauge bosons VV, such as WW, ZZ, Zγ,

$\gamma\gamma$, and gg are parameterized by a scattering amplitude that includes three tensor structures with expansion of coefficients up to (q^2/Λ^2):

$$A(\mathrm{HVV}) \sim \left[a_1^{\mathrm{VV}} + \frac{\kappa_1^{\mathrm{VV}} q_1^2 + \kappa_2^{\mathrm{VV}} q_2^2}{\left(\Lambda_1^{\mathrm{VV}}\right)^2}\right] m_{\mathrm{V1}}^2 \epsilon_{\mathrm{V1}}^* \epsilon_{\mathrm{V2}}^* + a_2^{\mathrm{VV}} f_{\mu\nu}^{*(1)} f^{*(2)\mu\nu} + a_3^{\mathrm{VV}} f_{\mu\nu}^{*(1)} \tilde{f}^{*(2)\mu\nu}, \quad (2)$$

where q_i, ϵ_{Vi}, and m_{V1} are the four-momentum, polarization vector, and pole mass of the gauge boson, indexed by $i = 1, 2$. The gauge boson's field strength tensor and dual field strength tensor are $f^{(i)\mu\nu} = \epsilon_{\mathrm{V}i}^{\mu} q_i^{\nu} - \epsilon_{\mathrm{V}i}^{\nu} q_i^{\mu}$ and $\tilde{f}_{\mu\nu}^{(i)} = \frac{1}{2}\epsilon_{\mu\nu\rho\sigma} f^{(i)\rho\sigma}$. The coupling coefficients a_i^{VV}, which multiply the three tensor structures, and $\kappa_i^{\mathrm{VV}}/(\Lambda_1^{\mathrm{VV}})^2$, which multiply the next term in the q^2 expansion for the first tensor structure, are to be determined from data, where Λ_1 is the scale of beyond the SM (BSM) physics.

In Eq. (2), the only nonzero SM contributions at tree-level are a_1^{WW} and a_1^{ZZ}, which are assumed to be equal under custodial symmetry. All other ZZ and WW couplings are considered anomalous contributions, which are either due to BSM physics or small contributions arising in the SM due to loop effects and are not accessible with the current precision. As the event kinematics of the H boson production in WW fusion and in ZZ fusion are very similar, they are analyzed together assuming $a_i^{\mathrm{WW}} = a_i^{\mathrm{ZZ}}$ and $\kappa_i^{\mathrm{ZZ}}/\left(\Lambda_1^{\mathrm{ZZ}}\right)^2 = \kappa_i^{\mathrm{WW}}/\left(\Lambda_1^{\mathrm{WW}}\right)^2$. The results can be reinterpreted for any other relationship between the a_i^{WW} and a_i^{ZZ} couplings [17]. For convenience, we refer to these parameters as a_i, κ_i, and Λ_1, without the superscripts. Among the anomalous contributions, considerations of symmetry and gauge invariance require $\kappa_1^{\mathrm{ZZ}} = \kappa_2^{\mathrm{ZZ}} = -\exp(i\phi_{\Lambda 1}^{\mathrm{ZZ}})$, $\kappa_1^{\gamma\gamma} = \kappa_2^{\gamma\gamma} = 0$, $\kappa_1^{\mathrm{gg}} = \kappa_2^{\mathrm{gg}} = 0$, $\kappa_1^{\mathrm{Z}\gamma} = 0$, and $\kappa_2^{\mathrm{Z}\gamma} = -\exp(i\phi_{\Lambda 1}^{\mathrm{Z}\gamma})$, where $\phi_{\Lambda 1}^{\mathrm{VV}}$ is the phase of the corresponding coupling. In the case of the $\gamma\gamma$ and gg couplings, the only contributing terms are $a_2^{\gamma\gamma,\mathrm{gg}}$ and $a_3^{\gamma\gamma,\mathrm{gg}}$. The precision of the constraints on $a_2^{\gamma\gamma,\mathrm{Z}\gamma}$ and $a_3^{\gamma\gamma,\mathrm{Z}\gamma}$ is still not competitive with on-shell photon measurements in $\mathrm{H} \to \mathrm{Z}\gamma$ and $\mathrm{H} \to \gamma\gamma$ [13]. We therefore omit those measurements in this paper. The coupling a_2^{gg} refers to an SM-like contribution in the gluon fusion process, and a_3^{gg} corresponds to a CP-odd anomalous contribution. There are four other anomalous couplings targeted in this analysis: two from the first term of Eq. (2), $\Lambda_1^{\mathrm{ZZ}} = \Lambda_1^{\mathrm{WW}} = \Lambda_1$ and $\Lambda_1^{\mathrm{Z}\gamma}$; one coming from the second term, $a_2^{\mathrm{ZZ}} = a_2^{\mathrm{WW}} = a_2$; and one coming from the third term, $a_3^{\mathrm{ZZ}} = a_3^{\mathrm{WW}} = a_3$. The a_3 coupling corresponds to the CP-odd amplitude, and its presence together with a CP-even amplitude would imply CP violation.

It is convenient to measure the effective cross-section ratios f_{ai} rather than the anomalous couplings a_i themselves, as most uncertainties cancel in the ratio. Moreover, the effective fractions are conveniently bounded between 0 and 1, independent of the coupling convention. The effective fractional cross sections f_{ai} and phases ϕ_{ai} are defined as follows:

$$\begin{aligned}
f_{a3} &= \frac{|a_3|^2\sigma_3}{|a_1|^2\sigma_1 + |a_2|^2\sigma_2 + |a_3|^2\sigma_3 + \tilde{\sigma}_{\Lambda 1}/\left(\Lambda_1\right)^4 + \ldots}, & \phi_{a3} &= \arg\left(\frac{a_3}{a_1}\right), \\
f_{a2} &= \frac{|a_2|^2\sigma_2}{|a_1|^2\sigma_1 + |a_2|^2\sigma_2 + |a_3|^2\sigma_3 + \tilde{\sigma}_{\Lambda 1}/\left(\Lambda_1\right)^4 + \ldots}, & \phi_{a2} &= \arg\left(\frac{a_2}{a_1}\right), \\
f_{\Lambda 1} &= \frac{\tilde{\sigma}_{\Lambda 1}/\left(\Lambda_1\right)^4}{|a_1|^2\sigma_1 + |a_2|^2\sigma_2 + |a_3|^2\sigma_3 + \tilde{\sigma}_{\Lambda 1}/\left(\Lambda_1\right)^4 + \ldots}, & \phi_{\Lambda 1}, & \quad (3) \\
f_{\Lambda 1}^{\mathrm{Z}\gamma} &= \frac{\tilde{\sigma}_{\Lambda 1}^{\mathrm{Z}\gamma}/\left(\Lambda_1^{\mathrm{Z}\gamma}\right)^4}{|a_1|^2\sigma_1 + \tilde{\sigma}_{\Lambda 1}^{\mathrm{Z}\gamma}/\left(\Lambda_1^{\mathrm{Z}\gamma}\right)^4 + \ldots}, & \phi_{ai}^{\mathrm{Z}\gamma}, &
\end{aligned}$$

where σ_i is the cross section for the process corresponding to $a_i = 1$, and all other couplings are set to zero. Since the production cross sections depend on the parton distribution functions (PDFs), the definition with respect to the decay process is more convenient. The cross section ratios defined in the $H \to 2e2\mu$ decay analysis [12] are adopted. Their values are: $\sigma_1/\sigma_3 = 6.53$, $\sigma_1/\sigma_2 = 2.77$, $(\sigma_1/\tilde{\sigma}_{\Lambda 1}) \times \text{TeV}^4 = 1.47 \times 10^4$, and $(\sigma_1/\tilde{\sigma}_{\Lambda 1}^{Z\gamma}) \times \text{TeV}^4 = 5.80 \times 10^3$, as calculated using JHUGEN 7.0.2 event generator [26–29]. The ellipsis (...) in Eq. (3) indicates any other contribution not listed explicitly.

Anomalous effects in the $H \to \tau\tau$ decay and $t\bar{t}H$ production are described by the Hff couplings of the H boson to fermions, with generally two couplings κ_f and $\tilde{\kappa}_f$, *CP*-even and *CP*-odd, respectively. Similarly, if the gluon coupling Hgg is dominated by the top quark loop, it can be described with the κ_t and $\tilde{\kappa}_t$ parameters. However, since other heavy states may contribute to the loop, we consider the effective Hgg coupling using the more general parameterization given in Eq. (2) instead of explicitly including the quark loop. In particular, the effective cross section fraction in gluon fusion becomes:

$$f_{a3}^{ggH} = \frac{|a_3^{ggH}|^2}{|a_2^{ggH}|^2 + |a_3^{ggH}|^2}, \tag{4}$$

where the cross-section ratio $\sigma_2^{ggH}/\sigma_3^{ggH} = 1$ drops out from the equation following the coupling convention in Eq. (2).

Experimentally observable effects resulting from the above anomalous couplings are discussed in the next section. In this paper, anomalous HWW, HZZ, and HZγ couplings are considered in VBF and VH production, and anomalous Hgg couplings are considered in gluon fusion. Since *CP*-violating effects in electroweak (VBF and VH) and gluon fusion production modify the same kinematic distributions, both *CP*-sensitive parameters, f_{a3} and f_{a3}^{ggH}, are left unconstrained simultaneously. It has been checked that *CP* violation in $H \to \tau\tau$ decays would not affect these measurements.

Following the formalism discussed in this section, simulated samples of H boson events produced via anomalous HVV couplings (VBF, VH, gluon fusion in association with two jets) are generated using JHUGEN. The associated production in gluon fusion with two jets is affected by anomalous interactions, while the kinematics of the production with zero or one jets are not affected. The latter events are generated with POWHEG 2.0 [52–55], which is used for yield normalization of events selected with two jets and for description of event distributions in categories of events where the correlation of the two jets is not important. For the kinematics relevant to this analysis in VBF and VH production, the effects that appear at next-to-leading order (NLO) in QCD are well approximated by the leading order (LO) QCD matrix elements used in JHUGEN, combined with parton showering. The JHUGEN samples produced with the SM couplings are compared with the equivalent samples generated by the POWHEG event generator at NLO QCD, with parton showering applied in both cases, and the kinematic distributions are found to agree.

The PYTHIA 8.212 [56] event generator is used to model the H boson decay to τ leptons and the decays of the τ leptons. Both scalar and pseudoscalar $H \to \tau\tau$ decays and their interference have been modeled to confirm that the analysis does not depend on the decay model. The default samples are generated with the scalar hypothesis in decay. The PDFs used in the generators are NNPDF30 [57], with their precision matching that of the matrix elements. All MC samples are further processed through a dedicated simulation of the CMS detector based on GEANT4 [58].

To simulate processes with anomalous H boson couplings, for each type of anomalous coupling we generate events with both the pure anomalous term and its interference with the SM contribution in the production HVV interaction. This allows extraction of the various coupling components and their interference. The MELA package, based on JHUGEN matrix elements, permits application of weights to events in any sample to model any other HVV or Hff couplings with the same production mechanism. Reweighting enables one to increase the effective simulated event count by using all samples at once to describe any model, even if it has not been simulated. The MELA package also allows calculation of optimal discriminants for further analysis, as discussed in Section 5.

Simulated samples for the modeling of background processes and of the H boson signal processes with SM couplings are the same as those used for the observation of the H boson decay to a pair of τ leptons [24]. The MG5_aMC@NLO [59] generator is used for Z + jets and W + jets processes. They are simulated at leading order (LO) with the MLM jet matching and merging [60]. The MG5_aMC@NLO generator is also used for diboson production simulated at next-to-LO (NLO) with the FxFx jet matching and merging [61], whereas POWHEG 2.0 and 1.0 are used for $\mathrm{t\bar{t}}$ and single top quark production, respectively. The generators are interfaced with PYTHIA to model the parton showering and fragmentation. The PYTHIA parameters affecting the description of the underlying event are set to the CUETP8M1 tune [62].

5 Discriminant distributions

The full kinematic information for both production and decay of the H boson can be extracted from each event. This paper focuses on the production process, illustrated in Fig. 2. The techniques discussed below are similar to those used in earlier analyses by CMS, such as in Ref. [17].

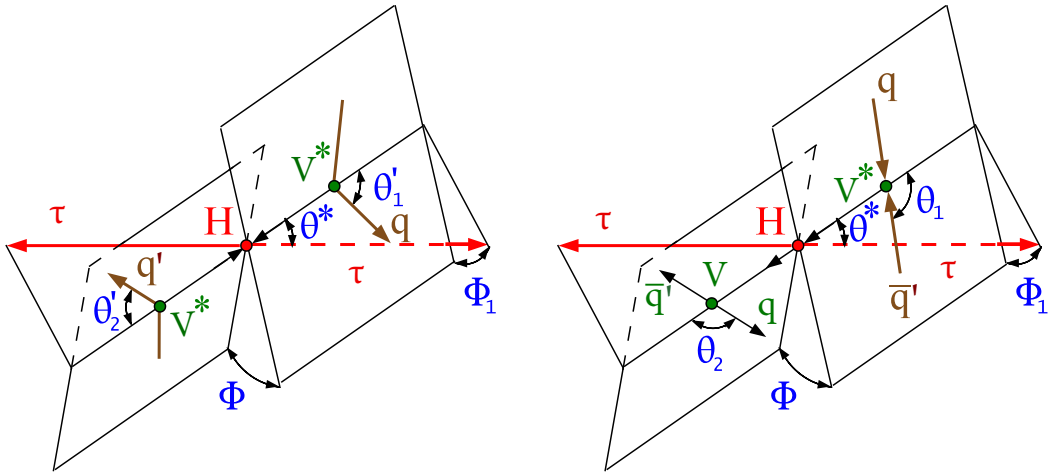

Figure 2: Illustrations of H boson production in $qq' \to gg(qq') \to H(qq') \to \tau\tau(qq')$ or VBF $qq' \to V^*V^*(qq') \to H(qq') \to \tau\tau(qq')$ (left) and in associated production $q\bar{q}' \to V^* \to VH \to q\bar{q}'\tau\tau$ (right). The $H \to \tau\tau$ decay is shown without further illustrating the τ decay chain. Angles and invariant masses fully characterize the orientation of the production and two-body decay chain and are defined in suitable rest frames of the V and H bosons, except in the VBF case, where only the H boson rest frame is used [26, 28].

The angular correlations between the two jets, the H boson, and the beamline direction in VBF, VH production, or gluon fusion production with an additional two jets provide sensitivity to quantum numbers and anomalous couplings of the H boson. A set of observables could be defined in VBF or VH production, such as $\vec{\Omega} = \{\theta_1, \theta_2, \Phi, \theta^*, \Phi_1, q_1^2, q_2^2\}$ for the VBF or

VH process with the angles illustrated in Fig. 2 and the q_1^2 and q_2^2 discussed in reference to Eq. (2), as described in detail in Ref. [28]. It is, however, a challenging task to perform an optimal analysis in a multidimensional space of observables. The MELA is designed to reduce the number of observables to the minimum while retaining all essential information for the purpose of a particular measurement. In this analysis, the background suppression is still provided by the observables defined in Ref. [24].

When the H boson and two associated jets are reconstructed, two types of discriminants can be used to optimally search for anomalous couplings. These two discriminants rely only on signal matrix elements and are well defined. One can apply the Neyman–Pearson lemma [63] to prove that the two discriminants constitute a minimal and complete set of optimal observables [28, 29] for the measurement of the f_{ai} parameter. One type of discriminant is designed to separate the process with anomalous couplings, denoted as BSM, from the SM signal process:

$$\mathcal{D}_{\rm BSM} = \frac{\mathcal{P}_{\rm SM}(\vec{\Omega})}{\mathcal{P}_{\rm SM}(\vec{\Omega}) + \mathcal{P}_{\rm BSM}(\vec{\Omega})}, \tag{5}$$

where $\mathcal{P}$ is the probability for the signal VBF production process (either SM or BSM), calculated using the matrix element MELA package and are normalized so that the matrix elements give the same cross sections for either $f_{ai} = 0$ or 1 in the relevant phase space of each process. Such a normalization leads to an optimal population of events in the range between 0 and 1. The discriminants are denoted as $\mathcal{D}_{0-}$, $\mathcal{D}_{0\mathrm{h}+}$, $\mathcal{D}_{\Lambda 1}$, or $\mathcal{D}_{\Lambda 1}^{\mathrm{Z}\gamma}$, depending on the targeted anomalous coupling a_3, a_2, Λ_1, or $\Lambda_1^{\mathrm{Z}\gamma}$, respectively.

The second type of discriminant targets the contribution from interference between the SM and BSM processes:

$$\mathcal{D}_{\rm int} = \frac{\mathcal{P}^{\rm int}_{\rm SM-BSM}(\vec{\Omega})}{\mathcal{P}_{\rm SM}(\vec{\Omega}) + \mathcal{P}_{\rm BSM}(\vec{\Omega})}, \tag{6}$$

where $\mathcal{P}^{\rm int}_{\rm SM-BSM}$ is the probability distribution for interference of SM and BSM signals in VBF production. This discriminant is used only for the CP-odd amplitude analysis with f_{a3} and is denoted $\mathcal{D}_{CP}$ in the rest of the paper. In the cases of $f_{\Lambda 1}$ and $f_{\Lambda 1}^{\mathrm{Z}\gamma}$, the interference discriminants do not carry additional information because of their high correlation with the $\mathcal{D}_{\Lambda 1}$ and $\mathcal{D}_{\Lambda 1}^{\mathrm{Z}\gamma}$ discriminants. The f_{a2} interference discriminant is not used in this analysis either, as it only becomes important for measurements of smaller couplings than presently tested and because of the limited number of events available for background parameterization.

Kinematic distributions of associated particles in gluon fusion are also sensitive to the quantum numbers of the H boson and to anomalous Hgg couplings. A set of observables, $\vec{\Omega}$, identical to those from the VBF process also describes this process. In this analysis, the focus is on the VBF-enhanced phase space in which the selection efficiency for the gluon fusion process is relatively small. Furthermore, the observables defined in Eqs. (5) and (6) for the VBF process are found to provide smaller separation between CP-even and CP-odd H boson couplings for gluon fusion production than MELA discriminants that would be dedicated to the gluon fusion process. Nonetheless, both parameters sensitive to CP violation, f_{a3} and f_{a3}^{ggH}, are included in a simultaneous fit using the observables optimized for the VBF process to avoid any possible bias in the measurement of f_{a3}.

While the correlations between the two jets, the H boson, and the beamline provide primary information about CP violation and anomalous couplings in electroweak production (VBF and VH), even events with reduced kinematic information can facilitate this analysis. For example,

in cases where both jets lie outside of the detector acceptance, the p_{T} distribution of the H boson is different for SM and BSM production. This leads to different event populations across the three categories and to a different p_{T} distribution of the H boson in the boosted category. For example, the fraction of signal events is much smaller in the 0-jet category and the p_{T} distribution is significantly harder in the boosted category for pseudoscalar H boson production than it is for the SM case. These effects are illustrated in Figs. 3, 4, and 5. The same effects are, however, negligible in gluon fusion production, where both scalar and pseudoscalar Hgg couplings are generated by higher-dimension operators, which correspond to the a_2^{gg} and a_3^{gg} terms in Eq. (2).

Other observables, such as $\Delta\Phi_{JJ}$ [43], defined as the azimuthal difference between the two associated jets, have been suggested for the study of CP effects. While they do provide sensitivity to CP measurements, they are not as sensitive as the discriminant variables for VBF production used in this analysis. Nonetheless, as an alternative to the optimal VBF analysis with the MELA discriminants, we also performed a cross-check analysis where the $\Delta\Phi_{JJ}$ observable is used instead. It was verified that the expected precision on f_{a3} is indeed lower than in the optimal VBF analysis. On the other hand, the sensitivity of the $\Delta\Phi_{JJ}$ observable to the f_{a3}^{ggH} parameter is better than that of the VBF discriminants, and it is close but not as good as the optimal MELA observables targeting the gluon fusion topology in association with two jets. Both results are discussed in Section 7.

6 Analysis implementation

Five anomalous HVV coupling parameters defined in Section 4 are studied: f_{a3}, f_{a2}, $f_{\Lambda1}$, $f_{\Lambda1}^{\mathrm{Z}\gamma}$, and f_{a3}^{ggH} describing anomalous couplings in VBF, VH, and gluon fusion production. The CP-sensitive parameters f_{a3} and f_{a3}^{ggH} are studied jointly, while all other parameters are examined independently. Anomalous H boson couplings in other production mechanisms and in the $\mathrm{H} \to \tau\tau$ decay do not affect these measurements, as the distributions studied here are insensitive to such effects.

The data, represented by a set of observables $\vec{x}$, is used to set constraints on anomalous coupling parameters. In the case of the CP study, the coupling parameters are f_{a3} and ϕ_{a3}. We also consider the scalar anomalous couplings described by f_{a2} and ϕ_{a2}; $f_{\Lambda1}$ and $\phi_{\Lambda1}$; and $f_{\Lambda1}^{\mathrm{Z}\gamma}$ and $\phi_{\Lambda1}^{\mathrm{Z}\gamma}$. Since only real couplings are considered, we fit for the products $f_{a3}\cos\phi_{a3}$ with $\cos\phi_{a3} = \pm1$, $f_{a2}\cos\phi_{a2}$ with $\cos\phi_{a2} = \pm1$, $f_{\Lambda1}\cos\phi_{\Lambda1}$ with $\cos\phi_{\Lambda1} = \pm1$, and $f_{\Lambda1}^{\mathrm{Z}\gamma}\cos\phi_{\Lambda1}^{\mathrm{Z}\gamma}$ with $\cos\phi_{\Lambda1}^{\mathrm{Z}\gamma} = \pm1$.

6.1 Observable distributions

Each event is described by its category k and the corresponding observables $\vec{x}$. In the 0-jet and boosted categories, which are dominated by the gluon fusion production mechanism, the observables are identical to those used in Ref. [24], namely $\vec{x} = \{m_{\mathrm{vis}}, M\}$ in the $\mathrm{e}\tau_{\mathrm{h}}$ and $\mu\tau_{\mathrm{h}}$ 0-jet categories, $\vec{x} = \{m_{\mathrm{vis}}, p_{\mathrm{T}}^{\mu}\}$ in the $\mathrm{e}\mu$ 0-jet category, $\vec{x} = \{m_{\tau\tau}\}$ in the 0-jet $\tau_{\mathrm{h}}\tau_{\mathrm{h}}$ category, and $\vec{x} = \{m_{\tau\tau}, p_{\mathrm{T}}^{\mathrm{H}}\}$ in the boosted categories, where M is the τ_{h} decay mode, p_{T}^{μ} is the transverse momentum of the muon, and $p_{\mathrm{T}}^{\mathrm{H}}$ is the transverse momentum of the H boson. There are no dedicated observables sensitive to anomalous couplings in these categories, as it is not possible to construct them in the absence of a correlated jet pair. Nonetheless, distributions of events in the above observables and categories still differ between signal models with variation of anomalous couplings.

In Figs. 3 and 4 the distributions of m_{vis} and $m_{\tau\tau}$ are displayed for selected events in the 0-jet category, and the transverse momentum distribution of the H boson is shown for the boosted category. Anomalous couplings would result in higher transverse momentum of the H boson and, unlike SM production, would cause the events to preferentially populate the boosted category instead of the one with no jets in the final state. The observable $m_{\tau\tau}$ is used in the $\tau_h\tau_h$ decay channel and m_{vis} in other channels in the 0-jet category. Two observables are used in the likelihood fit in the boosted category, $m_{\tau\tau}$ and p_T^H. In Fig. 3, the contribution from the $e\mu$ channel is omitted because of its low sensitivity and different binning in the fit. The normalization of the predicted background distributions corresponds to the result of the likelihood fit described in Section 6.2. In all production modes in Figs. 3 and 4, the $H \to \tau\tau$ process is normalized to its best-fit signal strength and couplings, and is shown as an open overlaid histogram. The background components labeled in the figures as "Others" include events from diboson and single top quark production, as well as H boson decays to W boson pairs. The uncertainty band accounts for all sources of uncertainty. The SM prediction for the VBF $H \to \tau\tau$ signal, multiplied by a factor 5000 (300) in Fig. 3 (4), is shown as a red open overlaid histogram. The black open overlaid histogram represents a BSM hypothesis for the VBF $H \to \tau\tau$ signal, normalized to 5000 (300) times the predicted SM cross section in Fig. 3 (4).

In Figs. 5–9, the discriminant distributions in the VBF category are displayed. In the VBF category, either three or four observables are used in the likelihood fit: $\vec{x} = \{m_{JJ}, m_{\tau\tau}, \mathcal{D}_{0-}, \mathcal{D}_{CP}\}$ are used to determine the f_{a3} parameter, $\vec{x} = \{m_{JJ}, m_{\tau\tau}, \mathcal{D}_{0h+}\}$ for the f_{a2} parameter, $\vec{x} = \{m_{JJ}, m_{\tau\tau}, \mathcal{D}_{\Lambda 1}\}$ for the $f_{\Lambda 1}$ parameter, and $\vec{x} = \{m_{JJ}, m_{\tau\tau}, \mathcal{D}_{\Lambda 1}^{Z\gamma}\}$ for the $f_{\Lambda 1}^{Z\gamma}$ parameter, as defined in Eqs. (5) and (6). In order to keep the background and signal templates sufficiently populated, a smaller number of bins is chosen for m_{JJ} and $m_{\tau\tau}$ compared to Ref. [24]. It was found that four bins in $\mathcal{D}_{0-}$, $\mathcal{D}_{0h+}$, $\mathcal{D}_{\Lambda 1}$, and $\mathcal{D}_{\Lambda 1}^{Z\gamma}$ are sufficient for close-to-optimal performance. At the same time, we adopt two bins in $\mathcal{D}_{CP}$ with $\mathcal{D}_{CP} < 0$ and $\mathcal{D}_{CP} > 0$. This choice does not lead to the need for additional bins in the templates, because all distributions except the CP-violating interference component are symmetric in $\mathcal{D}_{CP}$, and this symmetry is enforced in the templates. A forward-backward asymmetry in $\mathcal{D}_{CP}$ would be a clear indication of CP-sensitive effects and is present only in the signal interference template.

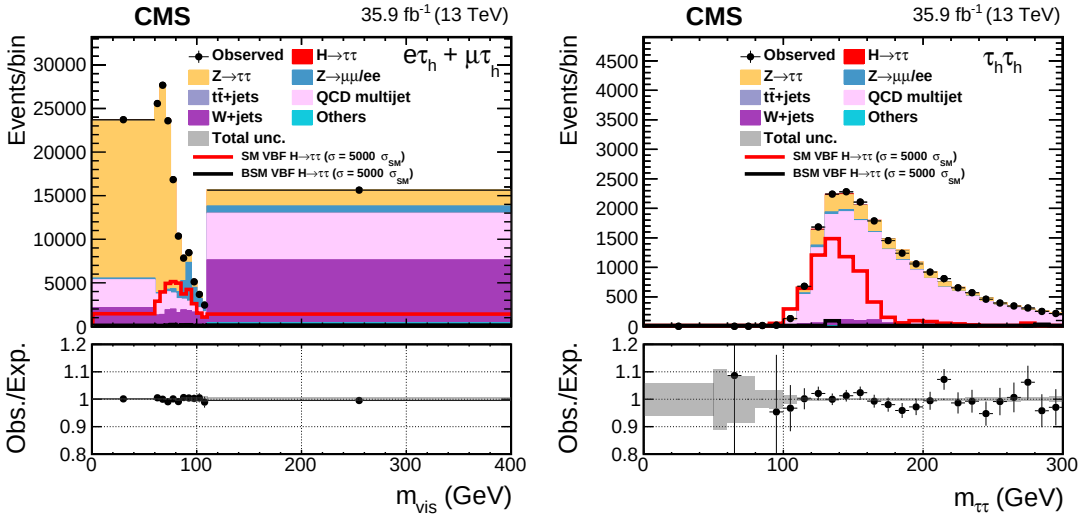

Figure 3: The distributions of m_{vis} and $m_{\tau\tau}$ in the 0-jet category of the $e\tau_h + \mu\tau_h$ (left) and $\tau_h\tau_h$ (right) decay channels. The BSM hypothesis corresponds to $f_{a3} = 1$.

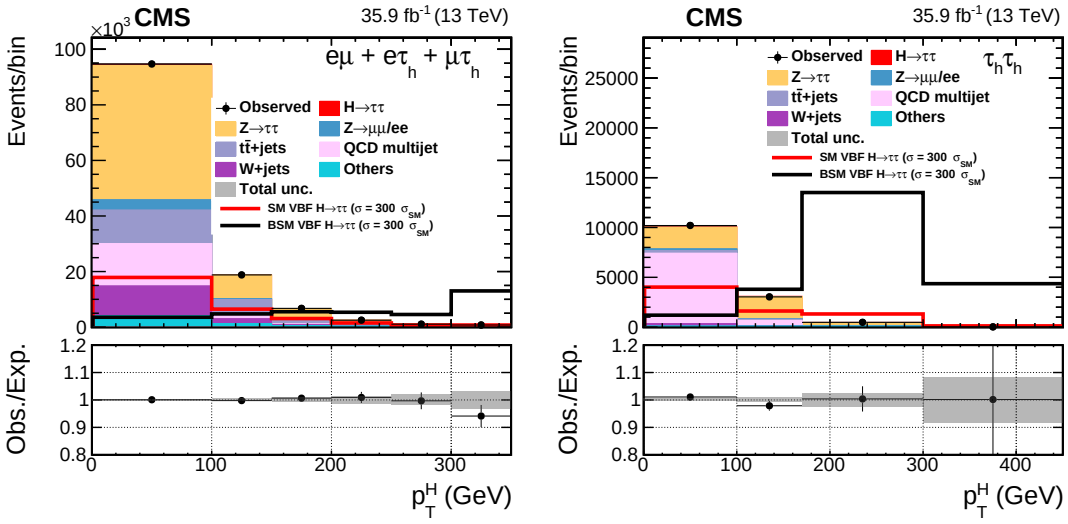

Figure 4: The distributions of transverse momentum of the H boson in the boosted category of the $e\tau_h + \mu\tau_h + e\mu$ (left) and $\tau_h\tau_h$ (right) decay channels. The BSM hypothesis corresponds to $f_{a3} = 1$.

6.2 Likelihood parameterization

We perform an unbinned extended maximum likelihood fit [64] to the events split into several categories according to the three production topologies and four tau-lepton pair final states using the RooFit toolkit [65, 66]. The probability density functions for signal $\mathcal{P}^{j,k}_{\text{sig}}(\vec{x})$ and background $\mathcal{P}^{j,k}_{\text{bkg}}(\vec{x})$ are binned templates and are defined for each production mechanism j in each category k. Each event is characterized by the discrete category k and up to four observables $\vec{x}$, depending on the category. For the VBF, VH, or gluon fusion production mechanisms, the signal probability density function is defined as

$$\mathcal{P}^{j,k}_{\text{sig}}(\vec{x}) = (1 - f_{ai})\, \mathcal{T}^{j,k}_{a1}(\vec{x}) + f_{ai}\, \mathcal{T}^{j,k}_{ai}(\vec{x}) + \sqrt{f_{ai}\,(1 - f_{ai})}\, \mathcal{T}^{j,k}_{a1,ai}(\vec{x}) \cos\phi_{ai}, \tag{7}$$

where $\mathcal{T}^{j,k}_{ai}$ is the template probability of a pure anomalous coupling a_i term and $\mathcal{T}^{j,k}_{a1,ai}$ describes the interference between the anomalous coupling and SM term a_1, or SM term a_2^{ggH} in the case of gluon fusion. Here f_{ai} stands for either f_{a3}, f_{a2}, $f_{\Lambda 1}$, $f_{\Lambda 1}^{Z\gamma}$, or f_{a3}^{ggH}. Each term in Eq. (7) is extracted from a dedicated simulation.

The signal strength parameters μ_V and μ_f are introduced as two parameters of interest. They scale the yields in the VBF+VH and gluon fusion production processes, respectively. They are defined such that for $f_{ai} = 0$ they are equal to the ratio of the measured cross section of the full process, including the $H \to \tau\tau$ decay, and the one expected in the SM, incorporating all the best known corrections. The likelihood is maximized with respect to the anomalous coupling $f_{ai}\cos\phi_{ai}$ and yield (μ_V, μ_f) parameters and with respect to the nuisance parameters, which include the constrained parameters describing the systematic uncertainties. The f_{a3} and f_{a3}^{ggH} parameters are tested simultaneously, while all other f_{ai} parameters are tested independently. All parameters except the anomalous coupling parameter of interest $f_{ai}\cos\phi_{ai}$ are profiled. The confidence level (CL) intervals are determined from profile likelihood scans of the respective parameters. The allowed 68 and 95% CL intervals are defined using the profile likelihood function, $-2\,\Delta\ln\mathcal{L} = 1.00$ and 3.84, respectively, for which exact coverage is expected in the asymptotic limit [67]. Approximate coverage has been tested with generated samples.

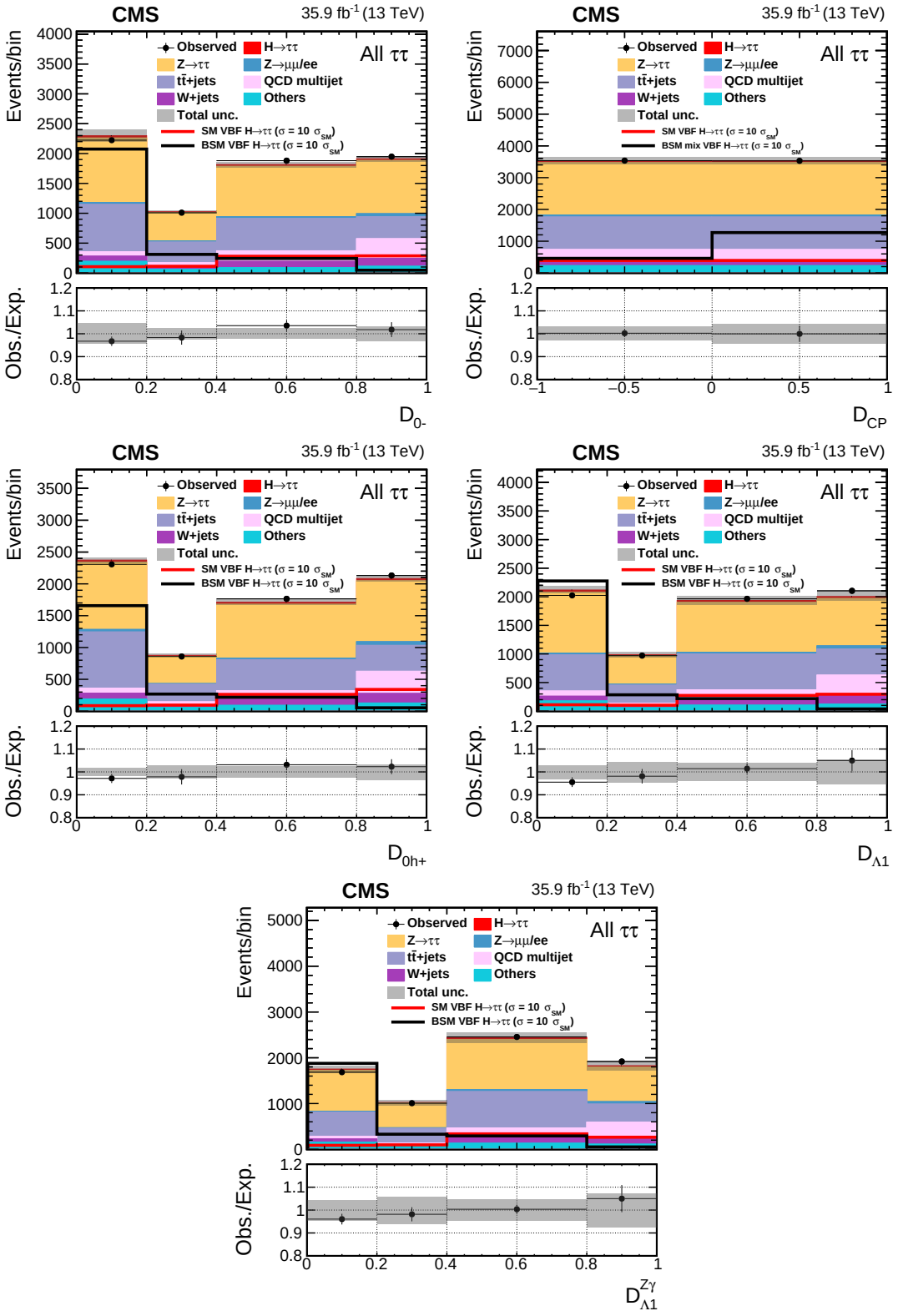

Figure 5: The distributions of $\mathcal{D}_{0-}$, $\mathcal{D}_{CP}$, $\mathcal{D}_{0h+}$, $\mathcal{D}_{\Lambda 1}$, and $\mathcal{D}_{\Lambda 1}^{Z\gamma}$ in the VBF category. All four decay channels, eμ, eτ_h, $\mu\tau_h$, and $\tau_h\tau_h$, are summed. The BSM hypothesis depends on the variable shown: it corresponds to $f_{a3} = 1$ for the $\mathcal{D}_{0-}$ (upper left) distributions, the maximal mixing ("BSM mix") in VBF production for the $\mathcal{D}_{CP}$ distribution (upper right), $f_{a2} = 1$ for the $\mathcal{D}_{0h+}$ distribution (middle left), $f_{\Lambda 1} = 1$ for the $\mathcal{D}_{\Lambda 1}$ distribution (middle right), and $f_{\Lambda 1}^{Z\gamma} = 1$ for the $\mathcal{D}_{\Lambda 1}^{Z\gamma}$ distribution (lower).

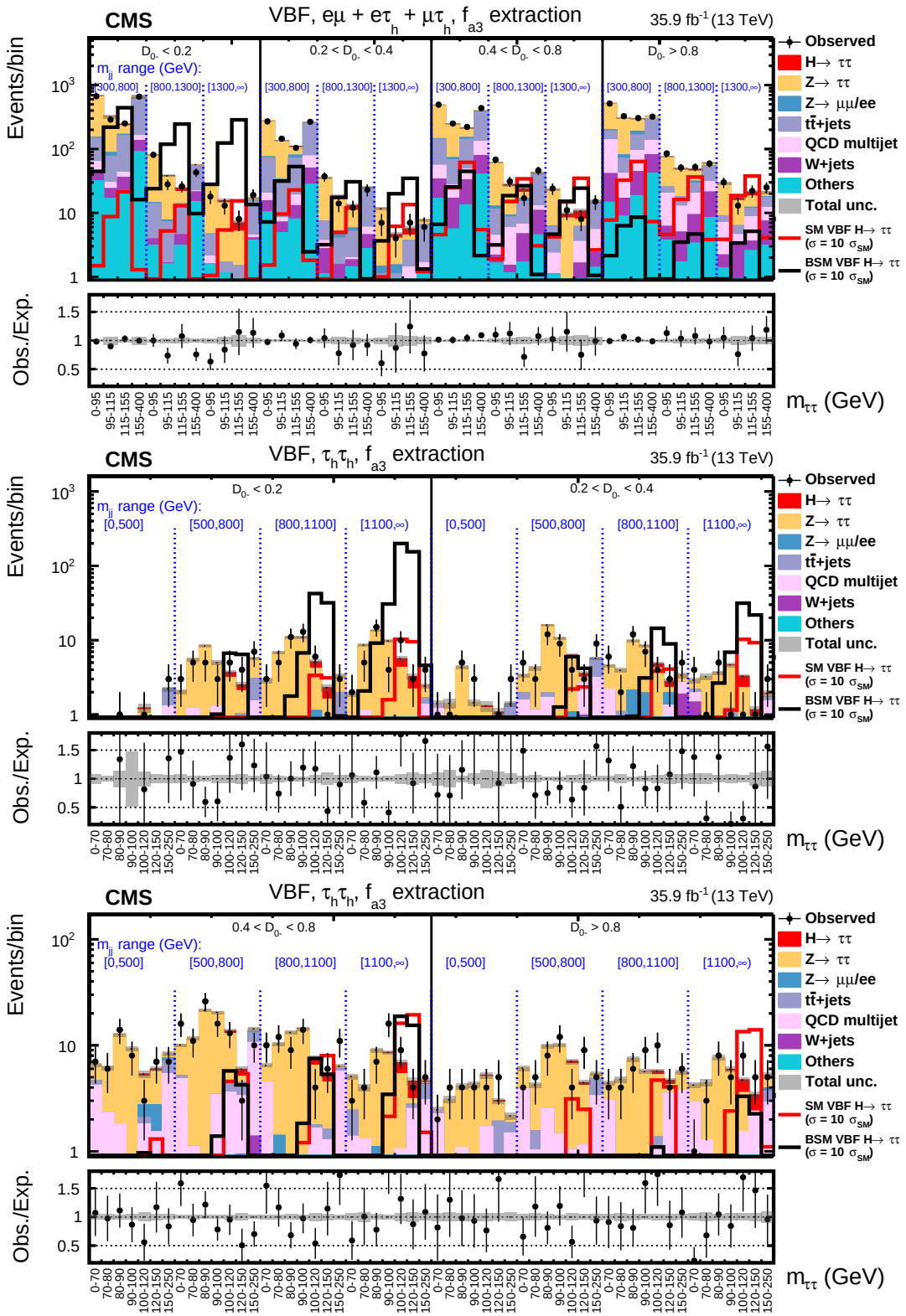

Figure 6: Observed and expected distributions in the VBF category in bins of $m_{\tau\tau}$, m_{JJ}, and $\mathcal{D}_{0-}$ in the f_{a3} analysis for the $e\mu + e\tau_h + \mu\tau_h$ (upper) and $\tau_h\tau_h$ (middle and lower) decay channels.

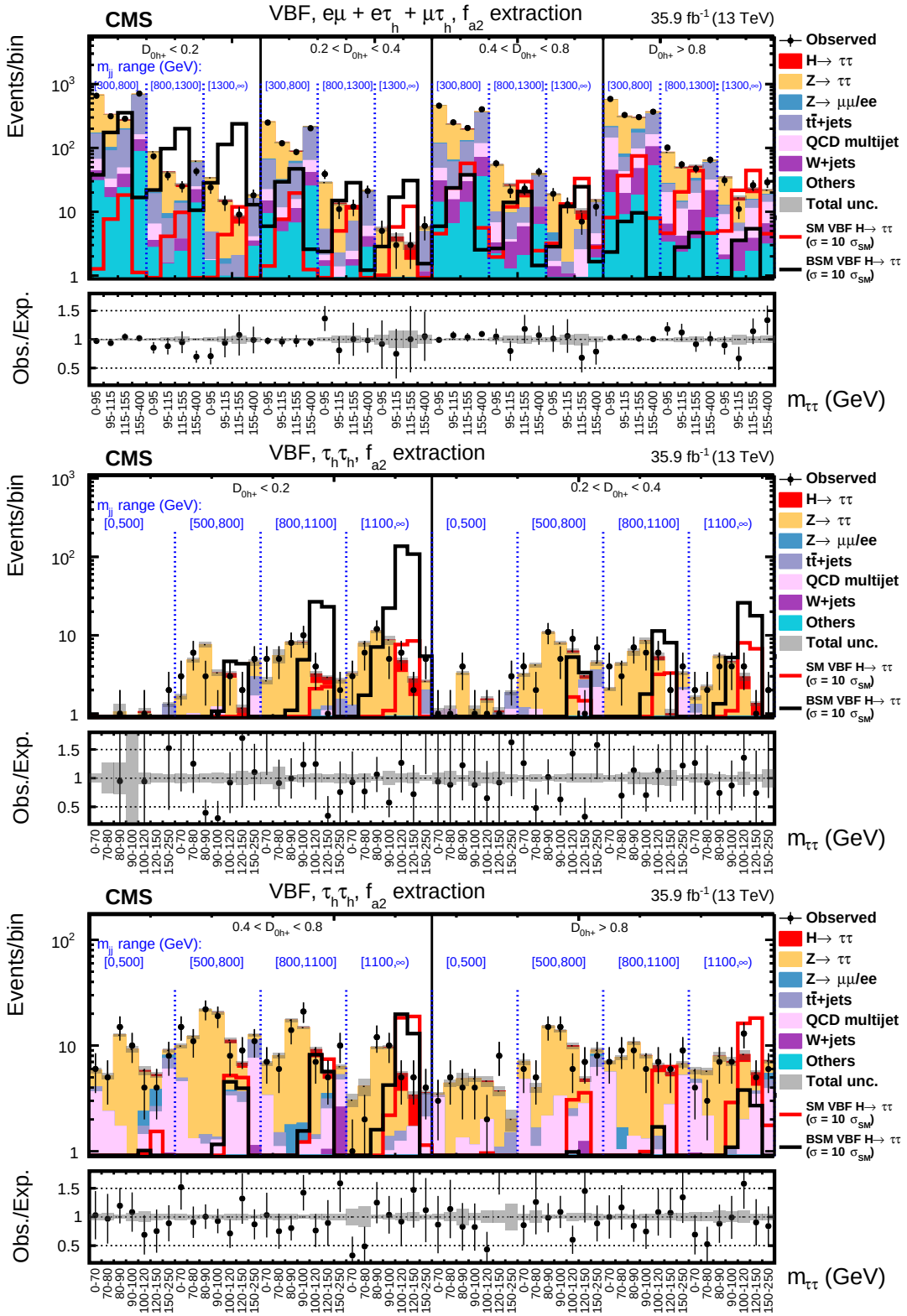

Figure 7: Observed and expected distributions in the VBF category in bins of $m_{\tau\tau}$, m_{JJ}, and $\mathcal{D}_{0h+}$ in the f_{a2} analysis for the $e\mu + e\tau_h + \mu\tau_h$ (upper) and $\tau_h\tau_h$ (middle and lower) decay channels.

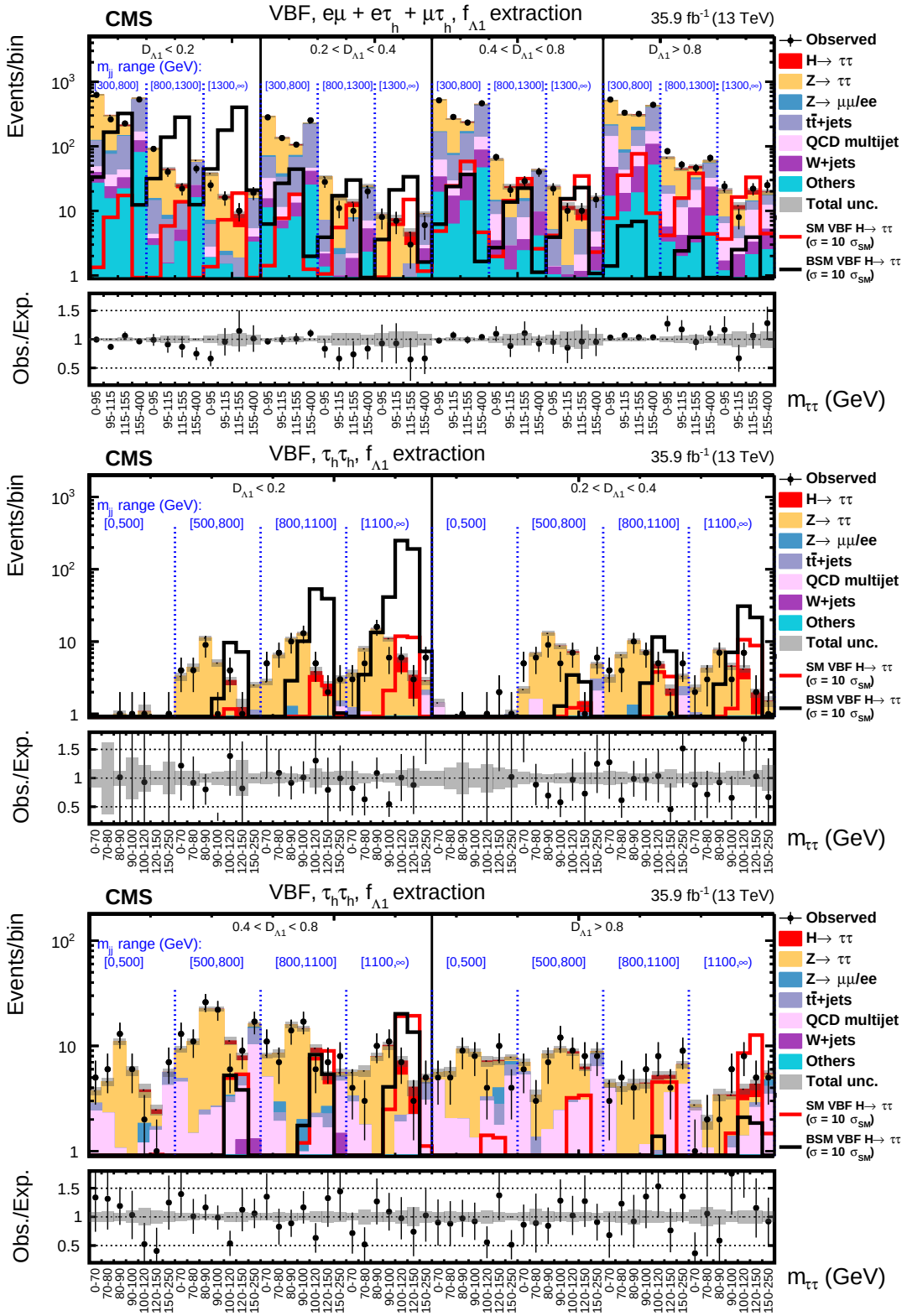

Figure 8: Observed and expected distributions in the VBF category in bins of $m_{\tau\tau}$, m_{JJ}, and $\mathcal{D}_{\Lambda 1}$ in the $f_{\Lambda 1}$ analysis for the $e\mu + e\tau_h + \mu\mu$ (upper) and $\tau_h\tau_h$ (middle and lower) decay channels.

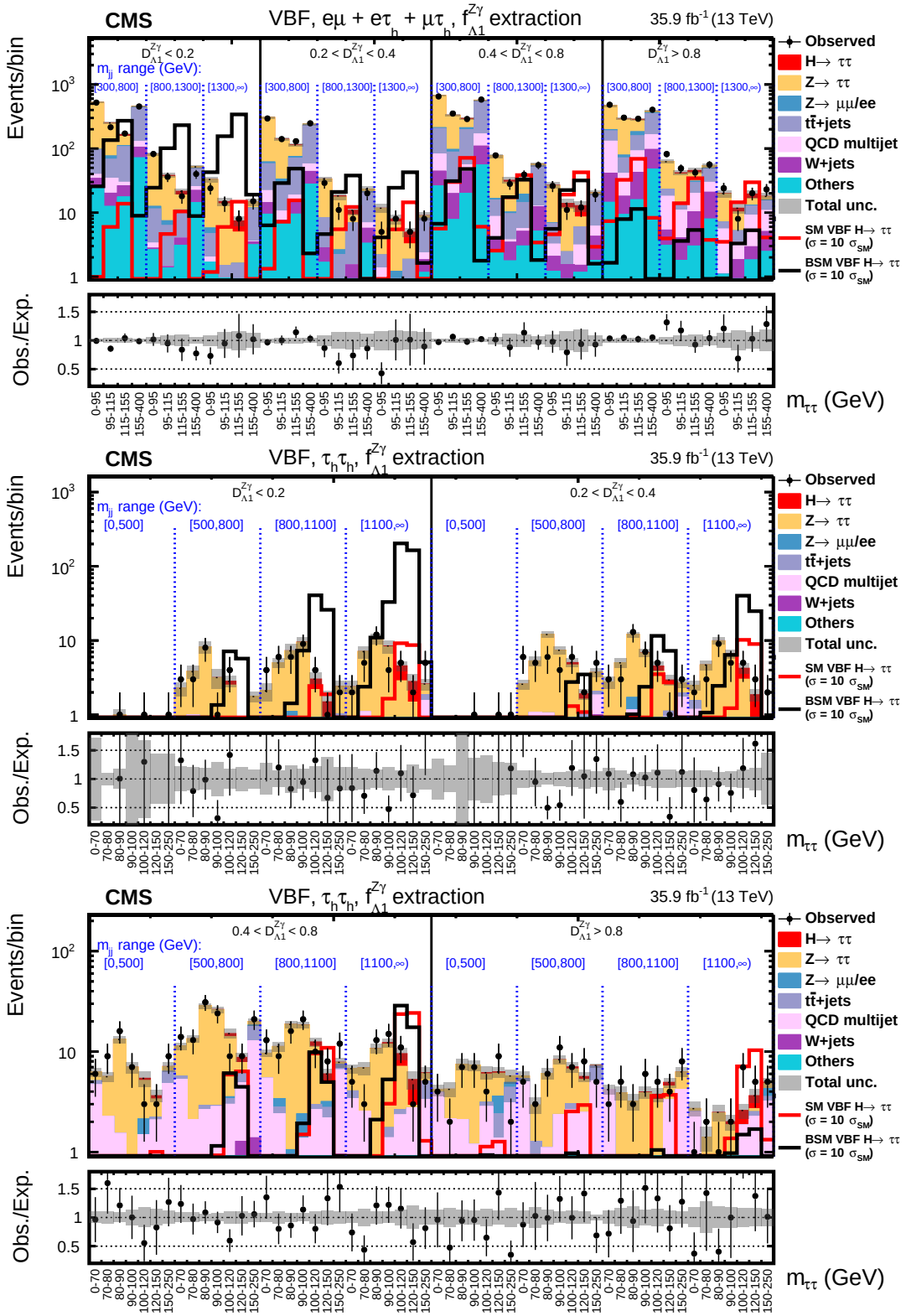

Figure 9: Observed and expected distributions in the VBF category in bins of $m_{\tau\tau}$, m_{JJ}, and $\mathcal{D}^{Z\gamma}_{\Lambda 1}$ in the $f^{Z\gamma}_{\Lambda 1}$ analysis for the $e\mu + e\tau_h + \tau_h\tau_h$ (upper) and $\tau_h\tau_h$ (middle and lower) decay channels.

6.3 Systematic uncertainties

A log-normal probability density function is assumed for the nuisance parameters that affect the event yields of the various background and signal contributions, whereas systematic uncertainties that affect the distributions are represented by nuisance parameters whose variation results in a continuous perturbation of the spectrum [68] and which are assumed to have a Gaussian probability density function. The systematic uncertainties are identical to those detailed in Ref. [24]. They are summarized in the following.

The rate uncertainties in the identification, isolation, and trigger efficiencies of electrons and muons amount to 2%. For τ_h, the uncertainty in the identification is 5% per τ_h candidate, and the uncertainty related to the trigger amounts to an additional 5% per τ_h candidate [39]. In the 0-jet category, where one of the dimensions of the 2D fit is the reconstructed τ_h decay mode, the relative reconstruction efficiency in a given τ_h reconstructed decay mode has an uncertainty of 3% [24]. For muons and electrons misreconstructed as τ_h candidates, the τ_h identification leads to rate uncertainties of 25 and 12%, respectively [39]. The requirement that there are no b-tagged jets in eμ decay channel events results in a rate uncertainty as large as 5% in the $\bar{t}t$ background [69].

The uncertainties in the energy scales of electrons, muons, and τ_h leptons amount to 1.0–2.5%, 1.0%, and 1.2%, respectively [39]. This uncertainty increases to 3.0 and 1.5%, respectively, for electrons and muons misidentified as τ_h candidates [24]. For events where quark- or gluon-initiated jets are misidentified as τ_h candidates, a linear uncertainty that increases by 20% per 100 GeV in transverse momentum of the τ_h and amounts to 20% for a τ_h with p_T of 100 GeV, is taken into account [24]. Uncertainties in the jet and p_T^{miss} energy scales are determined event-by-event [70], and propagated to the observables used in the analysis.

The uncertainty in the integrated luminosity is 2.5% [71]. Per bin uncertainties in the template probability parameterization related to the finite number of simulated events, or to the limited number of events in data control regions, are also taken into account [68].

The rate and acceptance uncertainties for the signal processes related to the theoretical calculations are due to uncertainties in the PDFs, variations of the renormalization and factorization scales, and uncertainties in the modeling of parton showers. The magnitude of the rate uncertainty depends on the production process and on the event category. In particular, the inclusive uncertainty related to the PDFs amounts 2.1% for the VBF production mode [72], while the corresponding uncertainty for the variation of the renormalization and factorization scales is 0.4% [72]. The acceptance uncertainties related to the particular selection criteria used in this analysis are less than 1% for all production modes. The theoretical uncertainty in the branching fraction of the H boson to τ leptons is 2.1% [72].

An overall rate uncertainty of 3–10% affects the $Z \to \tau\tau$ background, depending on the category, as estimated from a control region enriched in $Z \to \mu\mu$ events. In the VBF category, this process is also affected by a shape uncertainty that depends on m_{JJ} and $\Delta\Phi_{JJ}$, and can reach a magnitude of 20%. In addition to the uncertainties related to the W + jets control regions in the eτ_h and $\mu\tau_h$ final states, the W + jets background is affected by a rate uncertainty ranging between 5 and 10% to account for the extrapolation of the constraints from the high-m_T to the low-m_T regions. In the eμ and $\tau_h\tau_h$ final states, the rate uncertainty in the W + jets background yield is 20 and 4%, respectively.

The uncertainty in the QCD multijet background yield in the eμ decay channel ranges from 10 to 20%, depending on the category. In the eτ_h and $\mu\tau_h$ decay channels, uncertainties derived from the control regions are considered for the QCD multijet background, together with an ad-

ditional 20% uncertainty that accounts for the extrapolation from the relaxed-isolation control region to the isolated signal region. In the $\tau_h\tau_h$ decay channel, the uncertainty in the QCD multijet background yield is a combination of the uncertainties obtained from fitting the dedicated control regions with τ_h candidates passing relaxed isolation criteria, of the extrapolation to the signal region ranging from 3 to 15%, and of residual differences between prediction and data in signal-free regions with various loose isolation criteria.

The uncertainty from the fit in the $\mathrm{t\bar{t}}$ control region results in an uncertainty of about 5% on the $\mathrm{t\bar{t}}$ cross section in the signal region. The combined systematic uncertainty in the background yield arising from diboson and single top quark production processes is taken to be 5% [73, 74].

The additional $\mathcal{D}_{0-}$, $\mathcal{D}_{0h+}$, $\mathcal{D}_{\Lambda 1}$, and $\mathcal{D}_{\Lambda 1}^{Z\gamma}$ observables do not change the procedure for estimating the systematic uncertainty, as any mismodeling due to detector effects is estimated with the same procedure as for any other distribution. None of the systematic uncertainties introduce asymmetry in the $\mathcal{D}_{CP}$ distributions which remain symmetric, except for the antisymmetric signal interference contribution.

7 Results

The four sets of f_{ai} and ϕ_{ai} parameters describing anomalous HVV couplings, as defined in Eqs. (2) and (3), are tested against the data according to the probability density defined in Eq. (7). The results of the likelihood scans are shown in Fig. 10 and listed in Table 2. In each fit, the values of the other anomalous coupling parameters are set to zero. In the case of the *CP* fit, the f_{a3} parameter is measured simultaneously with f_{a3}^{ggH}, as defined in Eq. (4). All other parameters, including the signal strength parameters μ_V and μ_f, are profiled. The results are presented for the product of f_{ai} and $\cos(\phi_{ai})$, the latter being the sign of the real a_i/a_1 ratio of couplings. In this approach, the f_{ai} parameter is constrained to be in the physical range $f_{ai} \geq 0$. Therefore, in the SM it is likely for the best fit value to be at the physical boundary $f_{ai} = 0$.

Table 2: Allowed 68% CL (central values with uncertainties) and 95% CL (in square brackets) intervals on anomalous coupling parameters using the $H \to \tau\tau$ decay. The observed 95% CL constraints on $f_{a3}\cos(\phi_{a3})$ and $f_{a2}\cos(\phi_{a2})$ allow the full physics range $[-1, 1]$.

Parameter	Observed / (10^{-3})		Expected / (10^{-3})	
	68% CL	95% CL	68% CL	95% CL
$f_{a3}\cos(\phi_{a3})$	$0.00^{+0.93}_{-0.43}$	—	0.00 ± 0.28	$[-3.6, 3.6]$
$f_{a2}\cos(\phi_{a2})$	$0.0^{+1.2}_{-0.4}$	—	$0.0^{+2.0}_{-1.8}$	$[-10.0, 8.0]$
$f_{\Lambda 1}\cos(\phi_{\Lambda 1})$	$0.00^{+0.39}_{-0.10}$	$[-0.4, 1.8]$	$0.00^{+0.75}_{-0.16}$	$[-0.8, 3.6]$
$f_{\Lambda 1}^{Z\gamma}\cos(\phi_{\Lambda 1}^{Z\gamma})$	$0.0^{+1.2}_{-1.3}$	$[-7.4, 5.6]$	$0.0^{+3.0}_{-4.5}$	$[-19, 12]$

The constraints on f_{ai} appear relatively tight compared to similar constraints utilizing the H boson decay information, e.g. in Ref. [17]. This is because the cross section in VBF and VH production increases quickly with f_{ai}. The definition of f_{ai} in Eq. (3) uses the cross section ratios defined in the $H \to 2e2\mu$ decay as the common convention across various measurements. Because the cross section increases with respect to f_{ai} at different rates for production and decay, relatively small values of f_{ai} correspond to a substantial anomalous contribution to the production cross section. This leads to the plateau in the $-2\ln(\mathcal{L}/\mathcal{L}_{max})$ distributions for larger values of f_{ai} in Fig. 10. If we had used the cross section ratios for VBF production in the f_{ai} definition in Eq. (3), this plateau would not have been as pronounced. For example, the 68% CL

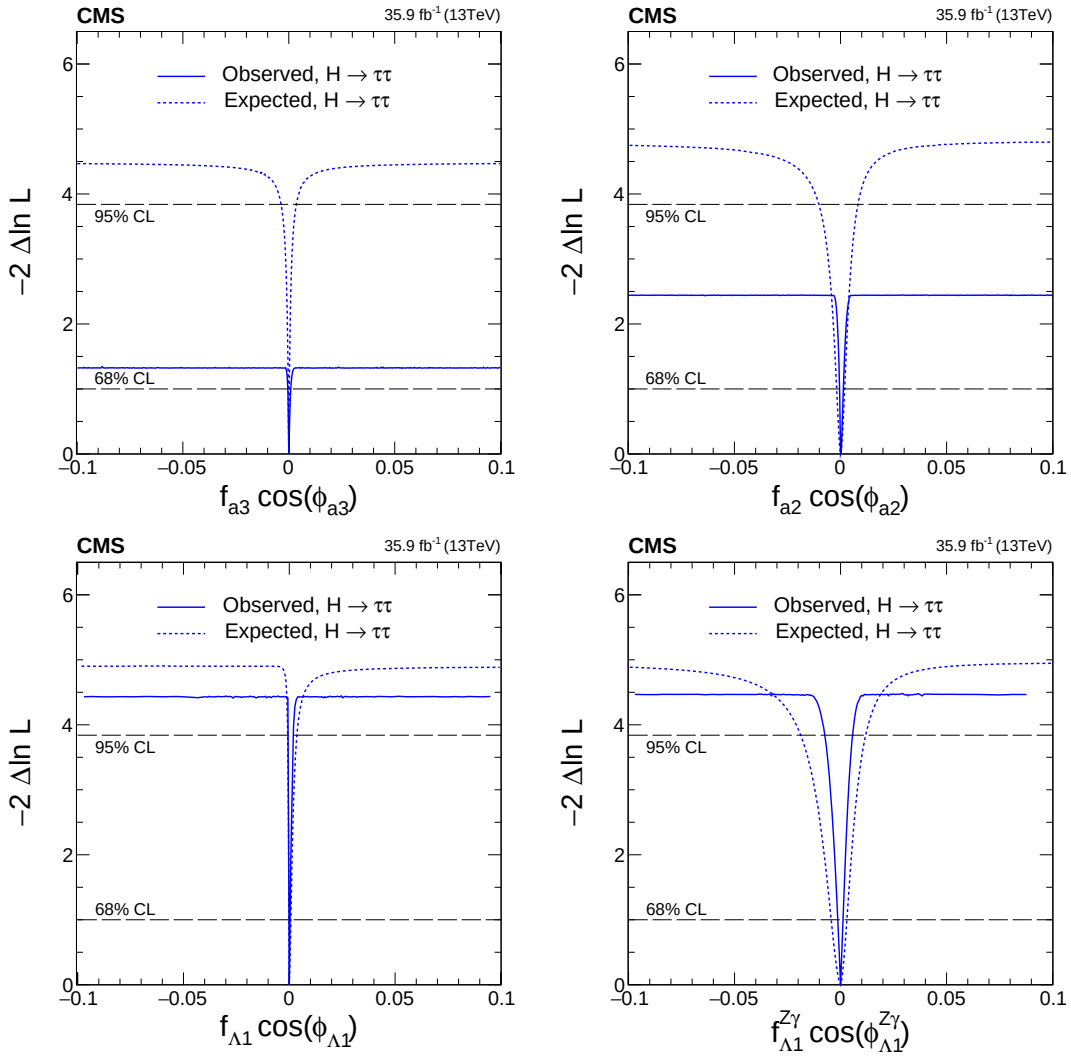

Figure 10: Observed (solid) and expected (dashed) likelihood scans of $f_{a3}\cos(\phi_{a3})$ (top left), $f_{a2}\cos(\phi_{a2})$ (top right), $f_{\Lambda 1}\cos(\phi_{\Lambda 1})$ (bottom left), and $f_{\Lambda 1}^{Z\gamma}\cos(\phi_{\Lambda 1}^{Z\gamma})$ (bottom right).

constraint on $f_{a3} < 0.00093$ is dominated by the VBF production information. If we were to use the VBF cross section ratio $\sigma_1^{\mathrm{VBF}}/\sigma_3^{\mathrm{VBF}} = 0.089$ in the f_{a3}^{VBF} definition in Eq. (3), this would correspond to the constraint $f_{a3}^{\mathrm{VBF}} < 0.064$ at 68% CL.

The observed maximum value of $-2\ln(\mathcal{L}/\mathcal{L}_{\max})$ is somewhat different from expectation and between the four analyses, mostly due to statistical fluctuations in the distribution of events across the dedicated discriminants and other observables, leading to different significances of the observed signal driven by VBF and VH production. In particular, the best-fit values for $(\mu_{\mathrm{V}}, \mu_{\mathrm{f}})$ in the four analyses, under the assumption that $f_{ai} = 0$ are: $(0.55 \pm 0.48, 1.03^{+0.45}_{-0.40})$ at $f_{a3} = 0$, $(0.72^{+0.48}_{-0.46}, 0.89^{+0.43}_{-0.37})$ at $f_{a2} = 0$, $(0.92^{+0.44}_{-0.45}, 0.82^{+0.46}_{-0.38})$ at $f_{\Lambda 1} = 0$, and $(0.94^{+0.48}_{-0.46}, 0.79 \pm 0.40)$ at $f_{\Lambda 1}^{Z\gamma} = 0$. This results in somewhat lower yield of VBF and VH events observed in the first two cases, leading to lower confidence levels in constraints on f_{a3} and f_{a2}.

In the f_{a3} analysis, a simultaneous measurement of f_{a3} and f_{a3}^{ggH} is performed. These are the parameters sensitive to CP in the VBF and gluon fusion processes, respectively. Both the observed and expected exclusions from the null hypothesis for any ggH BSM scenario with either MELA or the $\Delta\Phi_{JJ}$ observable are below one standard deviation.

8 Combination of results with other channels

The precision of the coupling measurements can be improved by combining the results in the $H \to \tau\tau$ channel, presented here, with those of other H boson decay channels. A combination is possible only with those channels where anomalous couplings in the VH, VBF, and gluon fusion processes are taken into account in the fit in a consistent way. If it is not done, the kinematics of the associated jets and of the H boson would not be modeled correctly for BSM values of the f_{ai} or f_{a3}^{ggH} parameters.

In the example of the CP fit, in the stand-alone fit with the $H \to \tau\tau$ channel, the parameters of interest are f_{a3}, f_{a3}^{ggH}, $\mu_V^{H\tau\tau}$, and $\mu_f^{H\tau\tau}$. When reporting one parameter, all other parameters are profiled. In a combined fit of the $H \to \tau\tau$ and $H \to VV$ channels, such as in Ref. [17], in principle there are four signal strength parameters in the two channels ($\mu_V^{H\tau\tau}$, $\mu_f^{H\tau\tau}$, μ_V^{HVV}, μ_f^{HVV}). However, this can be reduced to three parameters because the ratio between the VBF+VH and gluon fusion cross sections is expected to be the same in each of the two channels, that is $\mu_V^{H\tau\tau}/\mu_f^{H\tau\tau} = \mu_V^{HVV}/\mu_f^{HVV}$. Therefore, the three signal strength parameters are chosen as μ_V, μ_f, and η_τ, where the last one is the relative strength of the H boson coupling to the τ leptons. We should note that, as discussed earlier, the HWW couplings are analyzed together with the HZZ couplings assuming $a_i^{ZZ} = a_i^{WW}$. The results can be reinterpreted for a different assumption of the a_i^{ZZ}/a_i^{WW} ratio. In the combined likelihood fit, all common systematic uncertainties are correlated between the channels, both theoretical uncertainties, such as those due to the PDFs, and experimental uncertainties, such as jet energy calibration.

Table 3: Allowed 68% CL (central values with uncertainties) and 95% CL (in square brackets) intervals on anomalous coupling parameters using a combination of the $H \to \tau\tau$ and $H \to 4\ell$ [17] decay channels.

Parameter	Observed/(10^{-3})		Expected/(10^{-3})	
	68% CL	95% CL	68% CL	95% CL
$f_{a3}\cos(\phi_{a3})$	0.00 ± 0.27	$[-92, 14]$	0.00 ± 0.23	$[-1.2, 1.2]$
$f_{a2}\cos(\phi_{a2})$	$0.08^{+1.04}_{-0.21}$	$[-1.1, 3.4]$	$0.0^{+1.3}_{-1.1}$	$[-4.0, 4.2]$
$f_{\Lambda1}\cos(\phi_{\Lambda1})$	$0.00^{+0.53}_{-0.09}$	$[-0.4, 1.8]$	$0.00^{+0.48}_{-0.12}$	$[-0.5, 1.7]$
$f_{\Lambda1}^{Z\gamma}\cos(\phi_{\Lambda1}^{Z\gamma})$	$0.0^{+1.1}_{-1.3}$	$[-6.5, 5.7]$	$0.0^{+2.6}_{-3.6}$	$[-11, 8.0]$

The results using the $H \to \tau\tau$ decay are combined with those presented in Ref. [17] using the on-shell $H \to 4\ell$ decay. The latter employs results from Run 1 (from 2011 and 2012) and Run 2 (from 2015, 2016, and 2017) with data corresponding to integrated luminosities of 5.1, 19.7, and 80.2 fb^{-1} at center-of-mass energies 7, 8, and 13 TeV, respectively. In this analysis, information about HVV anomalous couplings both in VBF+VH production and in $H \to VV \to 4\ell$ decay is used. In all cases, the signal strength parameters are profiled, and the parameters common to the two analyses are correlated. The combined 68% CL and 95% CL intervals are presented in Table 3 and the likelihood scans are shown in Fig. 11. While the large confidence levels and large values of f_{ai} are predominantly constrained by the decay information in the $H \to VV$ analysis, the constraints in the narrow range of f_{ai} are dominated by the production information where the $H \to \tau\tau$ channel dominates over the $H \to 4\ell$, which results in the most stringent limits on anomalous HVV couplings. Reverting the transformation in Eq. (3) [17], the $f_{ai}\cos(\phi_{ai})$ results can be interpreted for the coupling parameters used in Eq. (2), as shown in Table 4.

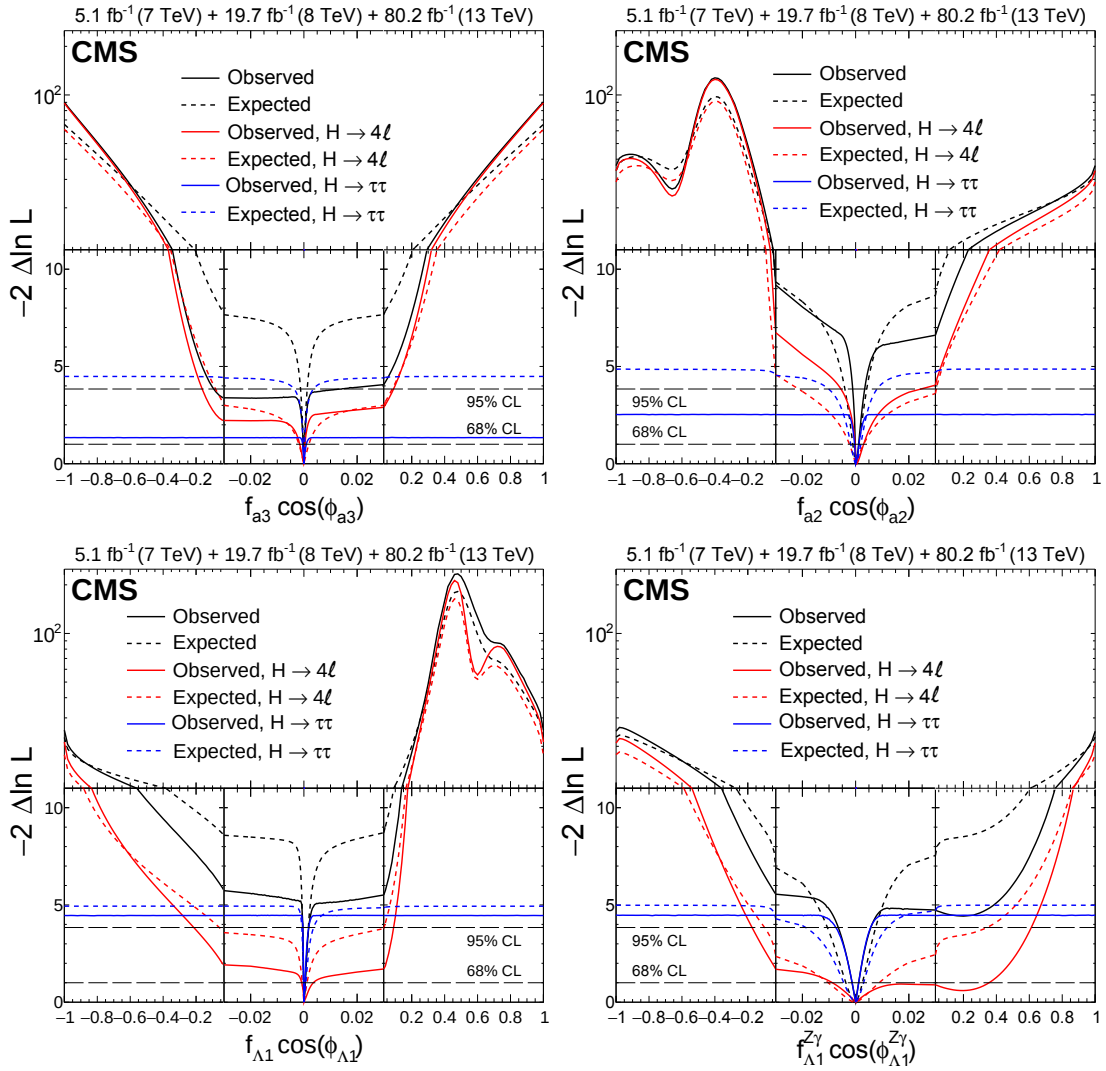

Figure 11: Combination of results using the $H \to \tau\tau$ decay (presented in this paper) and the $H \to 4\ell$ decay [17]. The observed (solid) and expected (dashed) likelihood scans of $f_{a3}\cos(\phi_{a3})$ (top left), $f_{a2}\cos(\phi_{a2})$ (top right), $f_{\Lambda 1}\cos(\phi_{\Lambda 1})$ (bottom left), and $f_{\Lambda 1}^{Z\gamma}\cos(\phi_{\Lambda 1}^{Z\gamma})$ (bottom right) are shown. For better visibility of all features, the x- and y-axes are presented with variable scales. On the linear-scale x-axis, a zoom is applied in the range -0.03 to 0.03. The y-axis is shown in linear (logarithmic) scale for values of $-2\,\Delta\ln\mathcal{L}$ below (above) 11.

9 Summary

A study is presented of anomalous HVV interactions of the H boson with vector bosons V, including CP violation, using its associated production with two hadronic jets in vector boson fusion, in the VH process, and in gluon fusion, and subsequently decaying to a pair of τ leptons. Constraints on the CP-violating parameter f_{a3} and on the CP-conserving parameters f_{a2}, $f_{\Lambda 1}$, and $f_{\Lambda 1}^{Z\gamma}$, defined in Eqs. (2) and (3), are set using matrix element techniques. The observed and expected limits on the parameters are summarized in Table 2. The 68% confidence level constraints are generally tighter than those from previous measurements using either production or decay information. Further constraints are obtained in the combination of the $H \to \tau\tau$ and $H \to 4\ell$ decay [17] channels and are summarized in Table 3. This combination places the most stringent constraints on anomalous H boson couplings: $f_{a3}\cos(\phi_{a3}) =$

Table 4: Summary of the allowed 95% CL intervals for the anomalous HVV couplings using the results in Table 3. The coupling ratios are assumed to be real and include the factor $\cos(\phi_{\Lambda 1})$ or $\cos(\phi_{\Lambda 1}^{Z\gamma}) = \pm 1$.

Parameter	Observed	Expected
a_3/a_1	$[-0.81, 0.31]$	$[-0.090, 0.090]$
a_2/a_1	$[-0.055, 0.097]$	$[-0.11, 0.11]$
$(\Lambda_1\sqrt{\lvert a_1\rvert})\cos(\phi_{\Lambda 1})$ (GeV)	$[-\infty, -650] \cup [440, \infty]$	$[-\infty, -610] \cup [450, \infty]$
$(\Lambda_1^{Z\gamma}\sqrt{\lvert a_1\rvert})\cos(\phi_{\Lambda 1}^{Z\gamma})$ (GeV)	$[-\infty, -400] \cup [420, \infty]$	$[-\infty, -360] \cup [390, \infty]$

$(0.00 \pm 0.27) \times 10^{-3}$, $f_{a2}\cos(\phi_{a2}) = (0.08^{+1.04}_{-0.21}) \times 10^{-3}$, $f_{\Lambda 1}\cos(\phi_{\Lambda 1}) = (0.00^{+0.53}_{-0.09}) \times 10^{-3}$, and $f_{\Lambda 1}^{Z\gamma}\cos(\phi_{\Lambda 1}^{Z\gamma}) = (0.0^{+1.1}_{-1.3}) \times 10^{-3}$. A simultaneous measurement of f_{a3} and f_{a3}^{ggH} parameters is performed, where the latter parameter, defined in Eqs. (2) and (4), is sensitive to CP violation effects in the gluon fusion process. The current data set does not allow for precise constraints on CP properties in the gluon fusion process. The results are consistent with expectations for the standard model H boson.

Acknowledgments

We thank Markus Schulze for optimizing the JHUGEN Monte Carlo simulation program and matrix element library for this analysis.

We congratulate our colleagues in the CERN accelerator departments for the excellent performance of the LHC and thank the technical and administrative staffs at CERN and at other CMS institutes for their contributions to the success of the CMS effort. In addition, we gratefully acknowledge the computing centers and personnel of the Worldwide LHC Computing Grid for delivering so effectively the computing infrastructure essential to our analyses. Finally, we acknowledge the enduring support for the construction and operation of the LHC and the CMS detector provided by the following funding agencies: BMBWF and FWF (Austria); FNRS and FWO (Belgium); CNPq, CAPES, FAPERJ, FAPERGS, and FAPESP (Brazil); MES (Bulgaria); CERN; CAS, MoST, and NSFC (China); COLCIENCIAS (Colombia); MSES and CSF (Croatia); RPF (Cyprus); SENESCYT (Ecuador); MoER, ERC IUT, and ERDF (Estonia); Academy of Finland, MEC, and HIP (Finland); CEA and CNRS/IN2P3 (France); BMBF, DFG, and HGF (Germany); GSRT (Greece); NKFIA (Hungary); DAE and DST (India); IPM (Iran); SFI (Ireland); INFN (Italy); MSIP and NRF (Republic of Korea); MES (Latvia); LAS (Lithuania); MOE and UM (Malaysia); BUAP, CINVESTAV, CONACYT, LNS, SEP, and UASLP-FAI (Mexico); MOS (Montenegro); MBIE (New Zealand); PAEC (Pakistan); MSHE and NSC (Poland); FCT (Portugal); JINR (Dubna); MON, RosAtom, RAS, RFBR, and NRC KI (Russia); MESTD (Serbia); SEIDI, CPAN, PCTI, and FEDER (Spain); MOSTR (Sri Lanka); Swiss Funding Agencies (Switzerland); MST (Taipei); ThEPCenter, IPST, STAR, and NSTDA (Thailand); TUBITAK and TAEK (Turkey); NASU and SFFR (Ukraine); STFC (United Kingdom); DOE and NSF (USA).

Individuals have received support from the Marie-Curie program and the European Research Council and Horizon 2020 Grant, contract Nos. 675440 and 765710 (European Union); the Leventis Foundation; the A.P. Sloan Foundation; the Alexander von Humboldt Foundation; the Belgian Federal Science Policy Office; the Fonds pour la Formation à la Recherche dans l'Industrie et dans l'Agriculture (FRIA-Belgium); the Agentschap voor Innovatie door Wetenschap en Technologie (IWT-Belgium); the F.R.S.-FNRS and FWO (Belgium) under the "Excellence of Science – EOS" – be.h project n. 30820817; the Beijing Municipal Science & Technology

Commission, No. Z181100004218003; the Ministry of Education, Youth and Sports (MEYS) of the Czech Republic; the Lendület ("Momentum") Program and the János Bolyai Research Scholarship of the Hungarian Academy of Sciences, the New National Excellence Program ÚNKP, the NKFIA research grants 123842, 123959, 124845, 124850, 125105, 128713, 128786, and 129058 (Hungary); the Council of Science and Industrial Research, India; the HOMING PLUS program of the Foundation for Polish Science, cofinanced from European Union, Regional Development Fund, the Mobility Plus program of the Ministry of Science and Higher Education, the National Science Center (Poland), contracts Harmonia 2014/14/M/ST2/00428, Opus 2014/13/B/ST2/02543, 2014/15/B/ST2/03998, and 2015/19/B/ST2/02861, Sonata-bis 2012/07/E/ST2/01406; the National Priorities Research Program by Qatar National Research Fund; the Programa Estatal de Fomento de la Investigación Científica y Técnica de Excelencia María de Maeztu, grant MDM-2015-0509 and the Programa Severo Ochoa del Principado de Asturias; the Thalis and Aristeia programs cofinanced by EU-ESF and the Greek NSRF; the Rachadapisek Sompot Fund for Postdoctoral Fellowship, Chulalongkorn University and the Chulalongkorn Academic into Its 2nd Century Project Advancement Project (Thailand); the Welch Foundation, contract C-1845; and the Weston Havens Foundation (USA).

References

[1] ATLAS Collaboration, "Observation of a new particle in the search for the Standard Model Higgs boson with the ATLAS detector at the LHC", *Phys. Lett. B* **716** (2012) 1, doi:10.1016/j.physletb.2012.08.020, arXiv:1207.7214.

[2] CMS Collaboration, "Observation of a new boson at a mass of 125 GeV with the CMS experiment at the LHC", *Phys. Lett. B* **716** (2012) 30, doi:10.1016/j.physletb.2012.08.021, arXiv:1207.7235.

[3] CMS Collaboration, "Observation of a new boson with mass near 125 GeV in pp collisions at $\sqrt{s}$ = 7 and 8 TeV", *JHEP* **06** (2013) 081, doi:10.1007/JHEP06(2013)081, arXiv:1303.4571.

[4] S. L. Glashow, "Partial-symmetries of weak interactions", *Nucl. Phys.* **22** (1961) 579, doi:10.1016/0029-5582(61)90469-2.

[5] F. Englert and R. Brout, "Broken Symmetry and the Mass of Gauge Vector Mesons", *Phys. Rev. Lett.* **13** (1964) 321, doi:10.1103/PhysRevLett.13.321.

[6] P. W. Higgs, "Broken symmetries, massless particles and gauge fields", *Phys. Lett.* **12** (1964) 132, doi:10.1016/0031-9163(64)91136-9.

[7] P. W. Higgs, "Broken symmetries and the masses of gauge bosons", *Phys. Rev. Lett.* **13** (1964) 508, doi:10.1103/PhysRevLett.13.508.

[8] G. S. Guralnik, C. R. Hagen, and T. W. B. Kibble, "Global conservation laws and massless particles", *Phys. Rev. Lett.* **13** (1964) 585, doi:10.1103/PhysRevLett.13.585.

[9] S. Weinberg, "A model of leptons", *Phys. Rev. Lett.* **19** (1967) 1264, doi:10.1103/PhysRevLett.19.1264.

[10] A. Salam, "Weak and electromagnetic interactions", in *Elementary particle physics: relativistic groups and analyticity*, N. Svartholm, ed., p. 367. Almqvist & Wiksell, Stockholm, 1968. Proceedings of the eighth Nobel symposium.

[11] CMS Collaboration, "On the mass and spin-parity of the Higgs boson candidate via its decays to Z boson pairs", *Phys. Rev. Lett.* **110** (2013) 081803, doi:10.1103/PhysRevLett.110.081803, arXiv:1212.6639.

[12] CMS Collaboration, "Measurement of the properties of a Higgs boson in the four-lepton final state", *Phys. Rev. D* **89** (2014) 092007, doi:10.1103/PhysRevD.89.092007, arXiv:1312.5353.

[13] CMS Collaboration, "Constraints on the spin-parity and anomalous HVV couplings of the Higgs boson in proton collisions at 7 and 8 TeV", *Phys. Rev. D* **92** (2015) 012004, doi:10.1103/PhysRevD.92.012004, arXiv:1411.3441.

[14] CMS Collaboration, "Limits on the Higgs boson lifetime and width from its decay to four charged leptons", *Phys. Rev. D* **92** (2015) 072010, doi:10.1103/PhysRevD.92.072010, arXiv:1507.06656.

[15] CMS Collaboration, "Combined search for anomalous pseudoscalar HVV couplings in VH(H $\to$ b$\bar{\text{b}}$) production and H $\to$ VV decay", *Phys. Lett. B* **759** (2016) 672, doi:10.1016/j.physletb.2016.06.004, arXiv:1602.04305.

[16] CMS Collaboration, "Constraints on anomalous Higgs boson couplings using production and decay information in the four-lepton final state", *Phys. Lett. B* **775** (2017) 1, doi:10.1016/j.physletb.2017.10.021, arXiv:1707.00541.

[17] CMS Collaboration, "Measurements of the Higgs boson width and anomalous HVV couplings from on-shell and off-shell production in the four-lepton final state", (2019). arXiv:1901.00174. Submitted to Phys. Rev. D.

[18] ATLAS Collaboration, "Evidence for the spin-0 nature of the Higgs boson using ATLAS data", *Phys. Lett. B* **726** (2013) 120, doi:10.1016/j.physletb.2013.08.026, arXiv:1307.1432.

[19] ATLAS Collaboration, "Study of the spin and parity of the Higgs boson in diboson decays with the ATLAS detector", *Eur. Phys. J. C* **75** (2015) 476, doi:10.1140/epjc/s10052-015-3685-1, arXiv:1506.05669.

[20] ATLAS Collaboration, "Test of CP invariance in vector-boson fusion production of the Higgs boson using the optimal observable method in the ditau decay channel with the ATLAS detector", *Eur. Phys. J. C* **76** (2016) 658, doi:10.1140/epjc/s10052-016-4499-5, arXiv:1602.04516.

[21] ATLAS Collaboration, "Measurement of inclusive and differential cross sections in the $H \to ZZ^* \to 4\ell$ decay channel in pp collisions at $\sqrt{s} = 13$ TeV with the ATLAS detector", *JHEP* **10** (2017) 132, doi:10.1007/JHEP10(2017)132, arXiv:1708.02810.

[22] ATLAS Collaboration, "Measurement of the Higgs boson coupling properties in the $H \to ZZ^* \to 4\ell$ decay channel at $\sqrt{s}$ = 13 TeV with the ATLAS detector", *JHEP* **03** (2018) 095, doi:10.1007/JHEP03(2018)095, arXiv:1712.02304.

[23] ATLAS Collaboration, "Measurements of Higgs boson properties in the diphoton decay channel with 36 fb^{-1} of pp collision data at $\sqrt{s} = 13$ TeV with the ATLAS detector", *Phys. Rev. D* **98** (2018) 052005, doi:10.1103/PhysRevD.98.052005, arXiv:1802.04146.

[24] CMS Collaboration, "Observation of the Higgs boson decay to a pair of τ leptons with the CMS detector", *Phys. Lett. B* **779** (2018) 283, doi:10.1016/j.physletb.2018.02.004, arXiv:1708.00373.

[25] S. Dawson et al., "Higgs working group report of the Snowmass 2013 community planning study", (2013). arXiv:1310.8361.

[26] Y. Gao et al., "Spin determination of single-produced resonances at hadron colliders", *Phys. Rev. D* **81** (2010) 075022, doi:10.1103/PhysRevD.81.075022, arXiv:1001.3396.

[27] S. Bolognesi et al., "Spin and parity of a single-produced resonance at the LHC", *Phys. Rev. D* **86** (2012) 095031, doi:10.1103/PhysRevD.86.095031, arXiv:1208.4018.

[28] I. Anderson et al., "Constraining anomalous HVV interactions at proton and lepton colliders", *Phys. Rev. D* **89** (2014) 035007, doi:10.1103/PhysRevD.89.035007, arXiv:1309.4819.

[29] A. V. Gritsan, R. Röntsch, M. Schulze, and M. Xiao, "Constraining anomalous Higgs boson couplings to the heavy flavor fermions using matrix element techniques", *Phys. Rev. D* **94** (2016) 055023, doi:10.1103/PhysRevD.94.055023, arXiv:1606.03107.

[30] CMS Collaboration, "The CMS trigger system", *JINST* **12** (2017) P01020, doi:10.1088/1748-0221/12/01/P01020, arXiv:1609.02366.

[31] CMS Collaboration, "The CMS experiment at the CERN LHC", *JINST* **3** (2008) S08004, doi:10.1088/1748-0221/3/08/S08004.

[32] CMS Collaboration, "Particle-flow reconstruction and global event description with the CMS detector", *JINST* **12** (2017) P10003, doi:10.1088/1748-0221/12/10/P10003, arXiv:1706.04965.

[33] M. Cacciari, G. P. Salam, and G. Soyez, "The anti-k_{T} jet clustering algorithm", *JHEP* **04** (2008) 063, doi:10.1088/1126-6708/2008/04/063, arXiv:0802.1189.

[34] M. Cacciari, G. P. Salam, and G. Soyez, "FastJet user manual", *Eur. Phys. J. C* **72** (2012) 1896, doi:10.1140/epjc/s10052-012-1896-2, arXiv:1111.6097.

[35] CMS Collaboration, "Performance of electron reconstruction and selection with the CMS detector in proton-proton collisions at $\sqrt{s} = 8$ TeV", *JINST* **10** (2015) P06005, doi:10.1088/1748-0221/10/06/P06005, arXiv:1502.02701.

[36] CMS Collaboration, "Performance of the CMS muon detector and muon reconstruction with proton-proton collisons at $\sqrt{s} = 13$ TeV", *JINST* **13** (2018) P06015, doi:10.1088/1748-0221/13/06/P06015, arXiv:1804.04528.

[37] M. Cacciari, G. P. Salam, "Dispelling the N^3 myth for the k_t jet-finder", *Phys. Lett. B* **641** (2006) 57, doi:10.1016/j.physletb.2006.08.037, arXiv:hep-ph/0512210.

[38] CMS Collaboration, "Reconstruction and identification of τ lepton decays to hadrons and ν_τ at CMS", *JINST* **11** (2016) P01019, doi:10.1088/1748-0221/11/01/P01019, arXiv:1510.07488.

[39] CMS Collaboration, "Performance of reconstruction and identification of τ leptons decaying to hadrons and ν_τ in pp collisions at $\sqrt{s} = 13$ TeV", *JINST* **13** (2018) P10005, doi:10.1088/1748-0221/13/10/P10005, arXiv:1809.02816.

[40] CMS Collaboration, "Performance of missing transverse momentum in pp collisions at $\sqrt{s} = 13\,\text{TeV}$ using the CMS detector", CMS Physics Analysis Summary CMS-PAS-JME-17-001, 2018.

[41] L. Bianchini, J. Conway, E. K. Friis, and C. Veelken, "Reconstruction of the Higgs mass in $H \to \tau\tau$ events by dynamical likelihood techniques", *J. Phys. Conf. Ser.* **513** (2014) 022035, doi:10.1088/1742-6596/513/2/022035.

[42] CMS Collaboration, "Search for neutral MSSM Higgs bosons decaying to a pair of tau leptons in pp collisions", *JHEP* **10** (2014) 160, doi:10.1007/JHEP10(2014)160, arXiv:1408.3316.

[43] T. Plehn, D. L. Rainwater, and D. Zeppenfeld, "Determining the structure of Higgs couplings at the LHC", *Phys. Rev. Lett.* **88** (2002) 051801, doi:10.1103/PhysRevLett.88.051801, arXiv:hep-ph/0105325.

[44] V. Hankele, G. Klamke, D. Zeppenfeld, and T. Figy, "Anomalous Higgs boson couplings in vector boson fusion at the CERN LHC", *Phys. Rev. D* **74** (2006) 095001, doi:10.1103/PhysRevD.74.095001, arXiv:hep-ph/0609075.

[45] E. Accomando et al., "Workshop on CP Studies and Non-Standard Higgs Physics", (2006). arXiv:hep-ph/0608079.

[46] K. Hagiwara, Q. Li, and K. Mawatari, "Jet angular correlation in vector-boson fusion processes at hadron colliders", *JHEP* **07** (2009) 101, doi:10.1088/1126-6708/2009/07/101, arXiv:0905.4314.

[47] A. De Rújula et al., "Higgs look-alikes at the LHC", *Phys. Rev. D* **82** (2010) 013003, doi:10.1103/PhysRevD.82.013003, arXiv:1001.5300.

[48] J. Ellis, D. S. Hwang, V. Sanz, and T. You, "A fast track towards the 'Higgs' spin and parity", *JHEP* **11** (2012) 134, doi:10.1007/JHEP11(2012)134, arXiv:1208.6002.

[49] P. Artoisenet et al., "A framework for Higgs characterisation", *JHEP* **11** (2013) 043, doi:10.1007/JHEP11(2013)043, arXiv:1306.6464.

[50] M. J. Dolan, P. Harris, M. Jankowiak, and M. Spannowsky, "Constraining CP-violating Higgs Sectors at the LHC using gluon fusion", *Phys. Rev. D* **90** (2014) 073008, doi:10.1103/PhysRevD.90.073008, arXiv:1406.3322.

[51] A. Greljo, G. Isidori, J. M. Lindert, and D. Marzocca, "Pseudo-observables in electroweak Higgs production", *Eur. Phys. J. C* **76** (2016) 158, doi:10.1140/epjc/s10052-016-4000-5, arXiv:1512.06135.

[52] S. Frixione, P. Nason, and C. Oleari, "Matching NLO QCD computations with parton shower simulations: the POWHEG method", *JHEP* **11** (2007) 070, doi:10.1088/1126-6708/2007/11/070, arXiv:0709.2092.

[53] E. Bagnaschi, G. Degrassi, P. Slavich, and A. Vicini, "Higgs production via gluon fusion in the POWHEG approach in the SM and in the MSSM", *JHEP* **02** (2012) 088, doi:10.1007/JHEP02(2012)088, arXiv:1111.2854.

[54] P. Nason and C. Oleari, "NLO Higgs boson production via vector-boson fusion matched with shower in POWHEG", *JHEP* **02** (2010) 037, doi:10.1007/JHEP02(2010)037, arXiv:0911.5299.

[55] G. Luisoni, P. Nason, C. Oleari, and F. Tramontano, "$HW^{\pm}$/HZ + 0 and 1 jet at NLO with the POWHEG BOX interfaced to GoSam and their merging within MiNLO", *JHEP* **10** (2013) 083, doi:10.1007/JHEP10(2013)083, arXiv:1306.2542.

[56] T. Sjostrand et al., "An introduction to PYTHIA 8.2", *Comput. Phys. Commun.* **191** (2015) 159, doi:10.1016/j.cpc.2015.01.024, arXiv:1410.3012.

[57] NNPDF Collaboration, "Unbiased global determination of parton distributions and their uncertainties at NNLO and at LO", *Nucl. Phys. B* **855** (2012) 153, doi:10.1016/j.nuclphysb.2011.09.024, arXiv:1107.2652.

[58] GEANT4 Collaboration, "GEANT4—a simulation toolkit", *Nucl. Instrum. Meth. A* **506** (2003) 250, doi:10.1016/S0168-9002(03)01368-8.

[59] J. Alwall et al., "The automated computation of tree-level and next-to-leading order differential cross sections, and their matching to parton shower simulations", *JHEP* **07** (2014) 079, doi:10.1007/JHEP07(2014)079, arXiv:1405.0301.

[60] J. Alwall et al., "Comparative study of various algorithms for the merging of parton showers and matrix elements in hadronic collisions", *Eur. Phys. J. C* **53** (2008) 473, doi:10.1140/epjc/s10052-007-0490-5, arXiv:0706.2569.

[61] R. Frederix and S. Frixione, "Merging meets matching in MC@NLO", *JHEP* **12** (2012) 061, doi:10.1007/JHEP12(2012)061, arXiv:1209.6215.

[62] CMS Collaboration, "Event generator tunes obtained from underlying event and multiparton scattering measurements", *Eur. Phys. J. C* **76** (2016) 155, doi:10.1140/epjc/s10052-016-3988-x, arXiv:1512.00815.

[63] J. Neyman and E. S. Pearson, "On the problem of the most efficient tests of statistical hypotheses", *Phil. Trans. R. Soc. Lond. A* **231** (1933) 289, doi:10.1098/rsta.1933.0009.

[64] R. J. Barlow, "Extended maximum likelihood", *Nucl. Instrum. Meth. A* **297** (1990) 496, doi:10.1016/0168-9002(90)91334-8.

[65] W. Verkerke and D. P. Kirkby, "The RooFit toolkit for data modeling", in *13^{th} International Conference for Computing in High-Energy and Nuclear Physics (CHEP03)*. 2003. arXiv:physics/0306116. CHEP-2003-MOLT007.

[66] R. Brun and F. Rademakers, "ROOT: An object oriented data analysis framework", *Nucl. Instrum. Meth. A* **389** (1997) 81, doi:10.1016/S0168-9002(97)00048-X.

[67] S. S. Wilks, "The large-sample distribution of the likelihood ratio for testing composite hypotheses", *Ann. Math. Stat.* **9** (1938) 60, doi:10.1214/aoms/1177732360.

[68] J. S. Conway, "Incorporating nuisance parameters in likelihoods for multisource spectra", in *Proceedings of PHYSTAT 2011 Workshop on Statistical Issues Related to Discovery Claims in Search Experiments and Unfolding*, p. 115. CERN-2011-006, 2011.

[69] CMS Collaboration, "Identification of heavy-flavour jets with the CMS detector in pp collisions at 13 TeV", *JINST* **13** (2018) P05011, doi:10.1088/1748-0221/13/05/P05011, arXiv:1712.07158.

[70] CMS Collaboration, "Performance of the CMS missing transverse momentum reconstruction in pp data at $\sqrt{s}$ = 8 TeV", *JINST* **10** (2015) P02006, doi:10.1088/1748-0221/10/02/P02006, arXiv:1411.0511.

[71] CMS Collaboration, "CMS luminosity measurements for the 2016 data taking period", CMS Physics Analysis Summary CMS-PAS-LUM-17-001, 2017.

[72] D. de Florian et al., "Handbook of LHC Higgs cross sections: 4. deciphering the nature of the Higgs sector", technical report, 2016. doi:10.23731/CYRM-2017-002, arXiv:1610.07922.

[73] CMS Collaboration, "Measurements of the pp $\to$ ZZ production cross section and the $Z \to 4\ell$ branching fraction, and constraints on anomalous triple gauge couplings at $\sqrt{s} = 13$ TeV", *Eur. Phys. J. C* **78** (2018) 165, doi:10.1140/epjc/s10052-018-5567-9, arXiv:1709.08601.

[74] CMS Collaboration, "Cross section measurement of t-channel single top quark production in pp collisions at $\sqrt{s} = 13$ TeV", *Phys. Lett. B* **772** (2017) 752, doi:10.1016/j.physletb.2017.07.047, arXiv:1610.00678.

A The CMS Collaboration

Yerevan Physics Institute, Yerevan, Armenia
A.M. Sirunyan, A. Tumasyan

Institut für Hochenergiephysik, Wien, Austria
W. Adam, F. Ambrogi, E. Asilar, T. Bergauer, J. Brandstetter, M. Dragicevic, J. Erö, A. Escalante Del Valle, M. Flechl, R. Frühwirth[1], V.M. Ghete, J. Hrubec, M. Jeitler[1], N. Krammer, I. Krätschmer, D. Liko, T. Madlener, I. Mikulec, N. Rad, H. Rohringer, J. Schieck[1], R. Schöfbeck, M. Spanring, D. Spitzbart, W. Waltenberger, J. Wittmann, C.-E. Wulz[1], M. Zarucki

Institute for Nuclear Problems, Minsk, Belarus
V. Chekhovsky, V. Mossolov, J. Suarez Gonzalez

Universiteit Antwerpen, Antwerpen, Belgium
E.A. De Wolf, D. Di Croce, X. Janssen, J. Lauwers, A. Lelek, M. Pieters, H. Van Haevermaet, P. Van Mechelen, N. Van Remortel

Vrije Universiteit Brussel, Brussel, Belgium
F. Blekman, J. D'Hondt, J. De Clercq, K. Deroover, G. Flouris, D. Lontkovskyi, S. Lowette, I. Marchesini, S. Moortgat, L. Moreels, Q. Python, K. Skovpen, S. Tavernier, W. Van Doninck, P. Van Mulders, I. Van Parijs

Université Libre de Bruxelles, Bruxelles, Belgium
D. Beghin, B. Bilin, H. Brun, B. Clerbaux, G. De Lentdecker, H. Delannoy, B. Dorney, G. Fasanella, L. Favart, A. Grebenyuk, A.K. Kalsi, J. Luetic, N. Postiau, E. Starling, L. Thomas, C. Vander Velde, P. Vanlaer, D. Vannerom, Q. Wang

Ghent University, Ghent, Belgium
T. Cornelis, D. Dobur, A. Fagot, M. Gul, I. Khvastunov[2], C. Roskas, D. Trocino, M. Tytgat, W. Verbeke, B. Vermassen, M. Vit, N. Zaganidis

Université Catholique de Louvain, Louvain-la-Neuve, Belgium
H. Bakhshiansohi, O. Bondu, G. Bruno, C. Caputo, P. David, C. Delaere, M. Delcourt, A. Giammanco, G. Krintiras, V. Lemaitre, A. Magitteri, K. Piotrzkowski, A. Saggio, M. Vidal Marono, P. Vischia, J. Zobec

Centro Brasileiro de Pesquisas Fisicas, Rio de Janeiro, Brazil
F.L. Alves, G.A. Alves, G. Correia Silva, C. Hensel, A. Moraes, M.E. Pol, P. Rebello Teles

Universidade do Estado do Rio de Janeiro, Rio de Janeiro, Brazil
E. Belchior Batista Das Chagas, W. Carvalho, J. Chinellato[3], E. Coelho, E.M. Da Costa, G.G. Da Silveira[4], D. De Jesus Damiao, C. De Oliveira Martins, S. Fonseca De Souza, L.M. Huertas Guativa, H. Malbouisson, D. Matos Figueiredo, M. Melo De Almeida, C. Mora Herrera, L. Mundim, H. Nogima, W.L. Prado Da Silva, L.J. Sanchez Rosas, A. Santoro, A. Sznajder, M. Thiel, E.J. Tonelli Manganote[3], F. Torres Da Silva De Araujo, A. Vilela Pereira

Universidade Estadual Paulista [a], Universidade Federal do ABC [b], São Paulo, Brazil
S. Ahuja[a], C.A. Bernardes[a], L. Calligaris[a], T.R. Fernandez Perez Tomei[a], E.M. Gregores[b], P.G. Mercadante[b], S.F. Novaes[a], SandraS. Padula[a]

Institute for Nuclear Research and Nuclear Energy, Bulgarian Academy of Sciences, Sofia, Bulgaria
A. Aleksandrov, R. Hadjiiska, P. Iaydjiev, A. Marinov, M. Misheva, M. Rodozov, M. Shopova, G. Sultanov

University of Sofia, Sofia, Bulgaria
A. Dimitrov, L. Litov, B. Pavlov, P. Petkov

Beihang University, Beijing, China
W. Fang[5], X. Gao[5], L. Yuan

Institute of High Energy Physics, Beijing, China
M. Ahmad, J.G. Bian, G.M. Chen, H.S. Chen, M. Chen, Y. Chen, C.H. Jiang, D. Leggat, H. Liao, Z. Liu, S.M. Shaheen[6], A. Spiezia, J. Tao, E. Yazgan, H. Zhang, S. Zhang[6], J. Zhao

State Key Laboratory of Nuclear Physics and Technology, Peking University, Beijing, China
Y. Ban, G. Chen, A. Levin, J. Li, L. Li, Q. Li, Y. Mao, S.J. Qian, D. Wang

Tsinghua University, Beijing, China
Y. Wang

Universidad de Los Andes, Bogota, Colombia
C. Avila, A. Cabrera, C.A. Carrillo Montoya, L.F. Chaparro Sierra, C. Florez, C.F. González Hernández, M.A. Segura Delgado

University of Split, Faculty of Electrical Engineering, Mechanical Engineering and Naval Architecture, Split, Croatia
N. Godinovic, D. Lelas, I. Puljak, T. Sculac

University of Split, Faculty of Science, Split, Croatia
Z. Antunovic, M. Kovac

Institute Rudjer Boskovic, Zagreb, Croatia
V. Brigljevic, D. Ferencek, K. Kadija, B. Mesic, M. Roguljic, A. Starodumov[7], T. Susa

University of Cyprus, Nicosia, Cyprus
M.W. Ather, A. Attikis, M. Kolosova, G. Mavromanolakis, J. Mousa, C. Nicolaou, F. Ptochos, P.A. Razis, H. Rykaczewski

Charles University, Prague, Czech Republic
M. Finger[8], M. Finger Jr.[8]

Escuela Politecnica Nacional, Quito, Ecuador
E. Ayala

Universidad San Francisco de Quito, Quito, Ecuador
E. Carrera Jarrin

Academy of Scientific Research and Technology of the Arab Republic of Egypt, Egyptian Network of High Energy Physics, Cairo, Egypt
A.A. Abdelalim[9,10], Y. Assran[11,12], M.A. Mahmoud[13,12]

National Institute of Chemical Physics and Biophysics, Tallinn, Estonia
S. Bhowmik, A. Carvalho Antunes De Oliveira, R.K. Dewanjee, K. Ehataht, M. Kadastik, M. Raidal, C. Veelken

Department of Physics, University of Helsinki, Helsinki, Finland
P. Eerola, H. Kirschenmann, J. Pekkanen, M. Voutilainen

Helsinki Institute of Physics, Helsinki, Finland
J. Havukainen, J.K. Heikkilä, T. Järvinen, V. Karimäki, R. Kinnunen, T. Lampén, K. Lassila-Perini, S. Laurila, S. Lehti, T. Lindén, P. Luukka, T. Mäenpää, H. Siikonen, E. Tuominen, J. Tuominiemi

Lappeenranta University of Technology, Lappeenranta, Finland
T. Tuuva

IRFU, CEA, Université Paris-Saclay, Gif-sur-Yvette, France
M. Besancon, F. Couderc, M. Dejardin, D. Denegri, J.L. Faure, F. Ferri, S. Ganjour, A. Givernaud, P. Gras, G. Hamel de Monchenault, P. Jarry, C. Leloup, E. Locci, J. Malcles, G. Negro, J. Rander, A. Rosowsky, M.Ö. Sahin, M. Titov

Laboratoire Leprince-Ringuet, Ecole polytechnique, CNRS/IN2P3, Université Paris-Saclay, Palaiseau, France
A. Abdulsalam[14], C. Amendola, I. Antropov, F. Beaudette, P. Busson, C. Charlot, B. Diab, R. Granier de Cassagnac, I. Kucher, A. Lobanov, J. Martin Blanco, C. Martin Perez, M. Nguyen, C. Ochando, G. Ortona, P. Paganini, J. Rembser, R. Salerno, J.B. Sauvan, Y. Sirois, A.G. Stahl Leiton, A. Zabi, A. Zghiche

Université de Strasbourg, CNRS, IPHC UMR 7178, Strasbourg, France
J.-L. Agram[15], J. Andrea, D. Bloch, G. Bourgatte, J.-M. Brom, E.C. Chabert, V. Cherepanov, C. Collard, E. Conte[15], J.-C. Fontaine[15], D. Gelé, U. Goerlach, M. Jansová, A.-C. Le Bihan, N. Tonon, P. Van Hove

Centre de Calcul de l'Institut National de Physique Nucleaire et de Physique des Particules, CNRS/IN2P3, Villeurbanne, France
S. Gadrat

Université de Lyon, Université Claude Bernard Lyon 1, CNRS-IN2P3, Institut de Physique Nucléaire de Lyon, Villeurbanne, France
S. Beauceron, C. Bernet, G. Boudoul, N. Chanon, R. Chierici, D. Contardo, P. Depasse, H. El Mamouni, J. Fay, S. Gascon, M. Gouzevitch, G. Grenier, B. Ille, F. Lagarde, I.B. Laktineh, H. Lattaud, M. Lethuillier, L. Mirabito, S. Perries, A. Popov[16], V. Sordini, G. Touquet, M. Vander Donckt, S. Viret

Georgian Technical University, Tbilisi, Georgia
A. Khvedelidze[8]

Tbilisi State University, Tbilisi, Georgia
Z. Tsamalaidze[8]

RWTH Aachen University, I. Physikalisches Institut, Aachen, Germany
C. Autermann, L. Feld, M.K. Kiesel, K. Klein, M. Lipinski, M. Preuten, M.P. Rauch, C. Schomakers, J. Schulz, M. Teroerde, B. Wittmer

RWTH Aachen University, III. Physikalisches Institut A, Aachen, Germany
A. Albert, M. Erdmann, S. Erdweg, T. Esch, R. Fischer, S. Ghosh, T. Hebbeker, C. Heidemann, K. Hoepfner, H. Keller, L. Mastrolorenzo, M. Merschmeyer, A. Meyer, P. Millet, S. Mukherjee, A. Novak, T. Pook, A. Pozdnyakov, M. Radziej, H. Reithler, M. Rieger, A. Schmidt, D. Teyssier, S. Thüer

RWTH Aachen University, III. Physikalisches Institut B, Aachen, Germany
G. Flügge, O. Hlushchenko, T. Kress, T. Müller, A. Nehrkorn, A. Nowack, C. Pistone, O. Pooth, D. Roy, H. Sert, A. Stahl[17]

Deutsches Elektronen-Synchrotron, Hamburg, Germany
M. Aldaya Martin, T. Arndt, C. Asawatangtrakuldee, I. Babounikau, K. Beernaert, O. Behnke, U. Behrens, A. Bermúdez Martínez, D. Bertsche, A.A. Bin Anuar, K. Borras[18], V. Botta, A. Campbell, P. Connor, C. Contreras-Campana, V. Danilov, A. De Wit, M.M. Defranchis, C. Diez Pardos, D. Domínguez Damiani, G. Eckerlin, T. Eichhorn, A. Elwood, E. Eren, E. Gallo[19], A. Geiser, J.M. Grados Luyando, A. Grohsjean, M. Guthoff, M. Haranko, A. Harb, H. Jung, M. Kasemann, J. Keaveney, C. Kleinwort, J. Knolle, D. Krücker, W. Lange, T. Lenz, J. Leonard, K. Lipka, W. Lohmann[20], R. Mankel, I.-A. Melzer-Pellmann, A.B. Meyer, M. Meyer, M. Missiroli, G. Mittag, J. Mnich, V. Myronenko, S.K. Pflitsch, D. Pitzl, A. Raspereza, A. Saibel, M. Savitskyi, P. Saxena, P. Schütze, C. Schwanenberger, R. Shevchenko, A. Singh, H. Tholen, O. Turkot, A. Vagnerini, M. Van De Klundert, G.P. Van Onsem, R. Walsh, Y. Wen, K. Wichmann, C. Wissing, O. Zenaiev

University of Hamburg, Hamburg, Germany
R. Aggleton, S. Bein, L. Benato, A. Benecke, V. Blobel, T. Dreyer, A. Ebrahimi, E. Garutti, D. Gonzalez, P. Gunnellini, J. Haller, A. Hinzmann, A. Karavdina, G. Kasieczka, R. Klanner, R. Kogler, N. Kovalchuk, S. Kurz, V. Kutzner, J. Lange, D. Marconi, J. Multhaup, M. Niedziela, C.E.N. Niemeyer, D. Nowatschin, A. Perieanu, A. Reimers, O. Rieger, C. Scharf, P. Schleper, S. Schumann, J. Schwandt, J. Sonneveld, H. Stadie, G. Steinbrück, F.M. Stober, M. Stöver, B. Vormwald, I. Zoi

Karlsruher Institut fuer Technologie, Karlsruhe, Germany
M. Akbiyik, C. Barth, M. Baselga, S. Baur, E. Butz, R. Caspart, T. Chwalek, F. Colombo, W. De Boer, A. Dierlamm, K. El Morabit, N. Faltermann, B. Freund, M. Giffels, M.A. Harrendorf, F. Hartmann[17], S.M. Heindl, U. Husemann, I. Katkov[16], S. Kudella, S. Mitra, M.U. Mozer, Th. Müller, M. Musich, M. Plagge, G. Quast, K. Rabbertz, M. Schröder, I. Shvetsov, H.J. Simonis, R. Ulrich, S. Wayand, M. Weber, T. Weiler, C. Wöhrmann, R. Wolf

Institute of Nuclear and Particle Physics (INPP), NCSR Demokritos, Aghia Paraskevi, Greece
G. Anagnostou, G. Daskalakis, T. Geralis, A. Kyriakis, D. Loukas, G. Paspalaki

National and Kapodistrian University of Athens, Athens, Greece
A. Agapitos, G. Karathanasis, P. Kontaxakis, A. Panagiotou, I. Papavergou, N. Saoulidou, K. Vellidis

National Technical University of Athens, Athens, Greece
G. Bakas, K. Kousouris, I. Papakrivopoulos, G. Tsipolitis

University of Ioánnina, Ioánnina, Greece
I. Evangelou, C. Foudas, P. Gianneios, P. Katsoulis, P. Kokkas, S. Mallios, K. Manitara, N. Manthos, I. Papadopoulos, E. Paradas, J. Strologas, F.A. Triantis, D. Tsitsonis

MTA-ELTE Lendület CMS Particle and Nuclear Physics Group, Eötvös Loránd University, Budapest, Hungary
M. Bartók[21], M. Csanad, N. Filipovic, P. Major, K. Mandal, A. Mehta, M.I. Nagy, G. Pasztor, O. Surányi, G.I. Veres

Wigner Research Centre for Physics, Budapest, Hungary
G. Bencze, C. Hajdu, D. Horvath[22], Á. Hunyadi, F. Sikler, T.Á. Vámi, V. Veszpremi, G. Vesztergombi†

Institute of Nuclear Research ATOMKI, Debrecen, Hungary
N. Beni, S. Czellar, J. Karancsi[21], A. Makovec, J. Molnar, Z. Szillasi

Institute of Physics, University of Debrecen, Debrecen, Hungary
P. Raics, Z.L. Trocsanyi, B. Ujvari

Indian Institute of Science (IISc), Bangalore, India
S. Choudhury, J.R. Komaragiri, P.C. Tiwari

National Institute of Science Education and Research, HBNI, Bhubaneswar, India
S. Bahinipati[24], C. Kar, P. Mal, A. Nayak[25], S. Roy Chowdhury, D.K. Sahoo[24], S.K. Swain

Panjab University, Chandigarh, India
S. Bansal, S.B. Beri, V. Bhatnagar, S. Chauhan, R. Chawla, N. Dhingra, R. Gupta, A. Kaur, M. Kaur, S. Kaur, P. Kumari, M. Lohan, M. Meena, K. Sandeep, S. Sharma, J.B. Singh, A.K. Virdi, G. Walia

University of Delhi, Delhi, India
A. Bhardwaj, B.C. Choudhary, R.B. Garg, M. Gola, S. Keshri, Ashok Kumar, S. Malhotra, M. Naimuddin, P. Priyanka, K. Ranjan, Aashaq Shah, R. Sharma

Saha Institute of Nuclear Physics, HBNI, Kolkata, India
R. Bhardwaj[26], M. Bharti[26], R. Bhattacharya, S. Bhattacharya, U. Bhawandeep[26], D. Bhowmik, S. Dey, S. Dutt[26], S. Dutta, S. Ghosh, M. Maity[27], K. Mondal, S. Nandan, A. Purohit, P.K. Rout, A. Roy, G. Saha, S. Sarkar, T. Sarkar[27], M. Sharan, B. Singh[26], S. Thakur[26]

Indian Institute of Technology Madras, Madras, India
P.K. Behera, A. Muhammad

Bhabha Atomic Research Centre, Mumbai, India
R. Chudasama, D. Dutta, V. Jha, V. Kumar, D.K. Mishra, P.K. Netrakanti, L.M. Pant, P. Shukla, P. Suggisetti

Tata Institute of Fundamental Research-A, Mumbai, India
T. Aziz, M.A. Bhat, S. Dugad, G.B. Mohanty, N. Sur, RavindraKumar Verma

Tata Institute of Fundamental Research-B, Mumbai, India
S. Banerjee, S. Bhattacharya, S. Chatterjee, P. Das, M. Guchait, Sa. Jain, S. Karmakar, S. Kumar, G. Majumder, K. Mazumdar, N. Sahoo

Indian Institute of Science Education and Research (IISER), Pune, India
S. Chauhan, S. Dube, V. Hegde, A. Kapoor, K. Kothekar, S. Pandey, A. Rane, A. Rastogi, S. Sharma

Institute for Research in Fundamental Sciences (IPM), Tehran, Iran
S. Chenarani[28], E. Eskandari Tadavani, S.M. Etesami[28], M. Khakzad, M. Mohammadi Najafabadi, M. Naseri, F. Rezaei Hosseinabadi, B. Safarzadeh[29], M. Zeinali

University College Dublin, Dublin, Ireland
M. Felcini, M. Grunewald

INFN Sezione di Bari [a], Università di Bari [b], Politecnico di Bari [c], Bari, Italy
M. Abbrescia[a,b], C. Calabria[a,b], A. Colaleo[a], D. Creanza[a,c], L. Cristella[a,b], N. De Filippis[a,c], M. De Palma[a,b], A. Di Florio[a,b], F. Errico[a,b], L. Fiore[a], A. Gelmi[a,b], G. Iaselli[a,c], M. Ince[a,b], S. Lezki[a,b], G. Maggi[a,c], M. Maggi[a], G. Miniello[a,b], S. My[a,b], S. Nuzzo[a,b], A. Pompili[a,b], G. Pugliese[a,c], R. Radogna[a], A. Ranieri[a], G. Selvaggi[a,b], A. Sharma[a], L. Silvestris[a], R. Venditti[a], P. Verwilligen[a]

INFN Sezione di Bologna [a], Università di Bologna [b], Bologna, Italy
G. Abbiendi[a], C. Battilana[a,b], D. Bonacorsi[a,b], L. Borgonovi[a,b], S. Braibant-Giacomelli[a,b], R. Campanini[a,b], P. Capiluppi[a,b], A. Castro[a,b], F.R. Cavallo[a], S.S. Chhibra[a,b], G. Codispoti[a,b], M. Cuffiani[a,b], G.M. Dallavalle[a], F. Fabbri[a], A. Fanfani[a,b], E. Fontanesi, P. Giacomelli[a], C. Grandi[a], L. Guiducci[a,b], F. Iemmi[a,b], S. Lo Meo[a,30], S. Marcellini[a], G. Masetti[a], A. Montanari[a], F.L. Navarria[a,b], A. Perrotta[a], F. Primavera[a,b], A.M. Rossi[a,b], T. Rovelli[a,b], G.P. Siroli[a,b], N. Tosi[a]

INFN Sezione di Catania [a], Università di Catania [b], Catania, Italy
S. Albergo[a,b,31], A. Di Mattia[a], R. Potenza[a,b], A. Tricomi[a,b,31], C. Tuve[a,b]

INFN Sezione di Firenze [a], Università di Firenze [b], Firenze, Italy
G. Barbagli[a], K. Chatterjee[a,b], V. Ciulli[a,b], C. Civinini[a], R. D'Alessandro[a,b], E. Focardi[a,b], G. Latino, P. Lenzi[a,b], M. Meschini[a], S. Paoletti[a], L. Russo[a,32], G. Sguazzoni[a], D. Strom[a], L. Viliani[a]

INFN Laboratori Nazionali di Frascati, Frascati, Italy
L. Benussi, S. Bianco, F. Fabbri, D. Piccolo

INFN Sezione di Genova [a], Università di Genova [b], Genova, Italy
F. Ferro[a], R. Mulargia[a,b], E. Robutti[a], S. Tosi[a,b]

INFN Sezione di Milano-Bicocca [a], Università di Milano-Bicocca [b], Milano, Italy
A. Benaglia[a], A. Beschi[b], F. Brivio[a,b], V. Ciriolo[a,b,17], S. Di Guida[a,b,17], M.E. Dinardo[a,b], S. Fiorendi[a,b], S. Gennai[a], A. Ghezzi[a,b], P. Govoni[a,b], M. Malberti[a,b], S. Malvezzi[a], D. Menasce[a], F. Monti, L. Moroni[a], M. Paganoni[a,b], D. Pedrini[a], S. Ragazzi[a,b], T. Tabarelli de Fatis[a,b], D. Zuolo[a,b]

INFN Sezione di Napoli [a], Università di Napoli 'Federico II' [b], Napoli, Italy, Università della Basilicata [c], Potenza, Italy, Università G. Marconi [d], Roma, Italy
S. Buontempo[a], N. Cavallo[a,c], A. De Iorio[a,b], A. Di Crescenzo[a,b], F. Fabozzi[a,c], F. Fienga[a], G. Galati[a], A.O.M. Iorio[a,b], L. Lista[a], S. Meola[a,d,17], P. Paolucci[a,17], C. Sciacca[a,b], E. Voevodina[a,b]

INFN Sezione di Padova [a], Università di Padova [b], Padova, Italy, Università di Trento [c], Trento, Italy
P. Azzi[a], N. Bacchetta[a], D. Bisello[a,b], A. Boletti[a,b], A. Bragagnolo, R. Carlin[a,b], P. Checchia[a], M. Dall'Osso[a,b], P. De Castro Manzano[a], T. Dorigo[a], U. Dosselli[a], F. Gasparini[a,b], U. Gasparini[a,b], A. Gozzelino[a], S.Y. Hoh, S. Lacaprara[a], P. Lujan, M. Margoni[a,b], A.T. Meneguzzo[a,b], J. Pazzini[a,b], M. Presilla[b], P. Ronchese[a,b], R. Rossin[a,b], F. Simonetto[a,b], A. Tiko, E. Torassa[a], M. Tosi[a,b], M. Zanetti[a,b], P. Zotto[a,b], G. Zumerle[a,b]

INFN Sezione di Pavia [a], Università di Pavia [b], Pavia, Italy
A. Braghieri[a], A. Magnani[a], P. Montagna[a,b], S.P. Ratti[a,b], V. Re[a], M. Ressegotti[a,b], C. Riccardi[a,b], P. Salvini[a], I. Vai[a,b], P. Vitulo[a,b]

INFN Sezione di Perugia [a], Università di Perugia [b], Perugia, Italy
M. Biasini[a,b], G.M. Bilei[a], C. Cecchi[a,b], D. Ciangottini[a,b], L. Fanò[a,b], P. Lariccia[a,b], R. Leonardi[a,b], E. Manoni[a], G. Mantovani[a,b], V. Mariani[a,b], M. Menichelli[a], A. Rossi[a,b], A. Santocchia[a,b], D. Spiga[a]

INFN Sezione di Pisa [a], Università di Pisa [b], Scuola Normale Superiore di Pisa [c], Pisa, Italy
K. Androsov[a], P. Azzurri[a], G. Bagliesi[a], L. Bianchini[a], T. Boccali[a], L. Borrello, R. Castaldi[a], M.A. Ciocci[a,b], R. Dell'Orso[a], G. Fedi[a], F. Fiori[a,c], L. Giannini[a,c], A. Giassi[a], M.T. Grippo[a], F. Ligabue[a,c], E. Manca[a,c], G. Mandorli[a,c], A. Messineo[a,b], F. Palla[a], A. Rizzi[a,b], G. Rolandi[33], P. Spagnolo[a], R. Tenchini[a], G. Tonelli[a,b], A. Venturi[a], P.G. Verdini[a]

INFN Sezione di Roma [a], Sapienza Università di Roma [b], Rome, Italy
L. Barone[a,b], F. Cavallari[a], M. Cipriani[a,b], D. Del Re[a,b], E. Di Marco[a,b], M. Diemoz[a], S. Gelli[a,b], E. Longo[a,b], B. Marzocchi[a,b], P. Meridiani[a], G. Organtini[a,b], F. Pandolfi[a], R. Paramatti[a,b], F. Preiato[a,b], S. Rahatlou[a,b], C. Rovelli[a], F. Santanastasio[a,b]

INFN Sezione di Torino [a], Università di Torino [b], Torino, Italy, Università del Piemonte Orientale [c], Novara, Italy
N. Amapane[a,b], R. Arcidiacono[a,c], S. Argiro[a,b], M. Arneodo[a,c], N. Bartosik[a], R. Bellan[a,b], C. Biino[a], A. Cappati[a,b], N. Cartiglia[a], F. Cenna[a,b], S. Cometti[a], M. Costa[a,b], R. Covarelli[a,b], N. Demaria[a], B. Kiani[a,b], C. Mariotti[a], S. Maselli[a], E. Migliore[a,b], V. Monaco[a,b], E. Monteil[a,b], M. Monteno[a], M.M. Obertino[a,b], L. Pacher[a,b], N. Pastrone[a], M. Pelliccioni[a], G.L. Pinna Angioni[a,b], A. Romero[a,b], M. Ruspa[a,c], R. Sacchi[a,b], R. Salvatico[a,b], K. Shchelina[a,b], V. Sola[a], A. Solano[a,b], D. Soldi[a,b], A. Staiano[a]

INFN Sezione di Trieste [a], Università di Trieste [b], Trieste, Italy
S. Belforte[a], V. Candelise[a,b], M. Casarsa[a], F. Cossutti[a], A. Da Rold[a,b], G. Della Ricca[a,b], F. Vazzoler[a,b], A. Zanetti[a]

Kyungpook National University, Daegu, Korea
D.H. Kim, G.N. Kim, M.S. Kim, J. Lee, S.W. Lee, C.S. Moon, Y.D. Oh, S.I. Pak, S. Sekmen, D.C. Son, Y.C. Yang

Chonnam National University, Institute for Universe and Elementary Particles, Kwangju, Korea
H. Kim, D.H. Moon, G. Oh

Hanyang University, Seoul, Korea
B. Francois, J. Goh[34], T.J. Kim

Korea University, Seoul, Korea
S. Cho, S. Choi, Y. Go, D. Gyun, S. Ha, B. Hong, Y. Jo, K. Lee, K.S. Lee, S. Lee, J. Lim, S.K. Park, Y. Roh

Sejong University, Seoul, Korea
H.S. Kim

Seoul National University, Seoul, Korea
J. Almond, J. Kim, J.S. Kim, H. Lee, K. Lee, S. Lee, K. Nam, S.B. Oh, B.C. Radburn-Smith, S.h. Seo, U.K. Yang, H.D. Yoo, G.B. Yu

University of Seoul, Seoul, Korea
D. Jeon, H. Kim, J.H. Kim, J.S.H. Lee, I.C. Park

Sungkyunkwan University, Suwon, Korea
Y. Choi, C. Hwang, J. Lee, I. Yu

Riga Technical University, Riga, Latvia
V. Veckalns[35]

Vilnius University, Vilnius, Lithuania
V. Dudenas, A. Juodagalvis, J. Vaitkus

National Centre for Particle Physics, Universiti Malaya, Kuala Lumpur, Malaysia
Z.A. Ibrahim, M.A.B. Md Ali[36], F. Mohamad Idris[37], W.A.T. Wan Abdullah, M.N. Yusli, Z. Zolkapli

Universidad de Sonora (UNISON), Hermosillo, Mexico
J.F. Benitez, A. Castaneda Hernandez, J.A. Murillo Quijada

Centro de Investigacion y de Estudios Avanzados del IPN, Mexico City, Mexico
H. Castilla-Valdez, E. De La Cruz-Burelo, M.C. Duran-Osuna, I. Heredia-De La Cruz[38], R. Lopez-Fernandez, J. Mejia Guisao, R.I. Rabadan-Trejo, G. Ramirez-Sanchez, R. Reyes-Almanza, A. Sanchez-Hernandez

Universidad Iberoamericana, Mexico City, Mexico
S. Carrillo Moreno, C. Oropeza Barrera, M. Ramirez-Garcia, F. Vazquez Valencia

Benemerita Universidad Autonoma de Puebla, Puebla, Mexico
J. Eysermans, I. Pedraza, H.A. Salazar Ibarguen, C. Uribe Estrada

Universidad Autónoma de San Luis Potosí, San Luis Potosí, Mexico
A. Morelos Pineda

University of Auckland, Auckland, New Zealand
D. Krofcheck

University of Canterbury, Christchurch, New Zealand
S. Bheesette, P.H. Butler

National Centre for Physics, Quaid-I-Azam University, Islamabad, Pakistan
A. Ahmad, M. Ahmad, M.I. Asghar, Q. Hassan, H.R. Hoorani, W.A. Khan, M.A. Shah, M. Shoaib, M. Waqas

National Centre for Nuclear Research, Swierk, Poland
H. Bialkowska, M. Bluj, B. Boimska, T. Frueboes, M. Górski, M. Kazana, M. Szleper, P. Traczyk, P. Zalewski

Institute of Experimental Physics, Faculty of Physics, University of Warsaw, Warsaw, Poland
K. Bunkowski, A. Byszuk[39], K. Doroba, A. Kalinowski, M. Konecki, J. Krolikowski, M. Misiura, M. Olszewski, A. Pyskir, M. Walczak

Laboratório de Instrumentação e Física Experimental de Partículas, Lisboa, Portugal
M. Araujo, P. Bargassa, C. Beirão Da Cruz E Silva, A. Di Francesco, P. Faccioli, B. Galinhas, M. Gallinaro, J. Hollar, N. Leonardo, J. Seixas, G. Strong, O. Toldaiev, J. Varela

Joint Institute for Nuclear Research, Dubna, Russia
S. Afanasiev, P. Bunin, M. Gavrilenko, I. Golutvin, I. Gorbunov, A. Kamenev, V. Karjavine, A. Lanev, A. Malakhov, V. Matveev[40,41], P. Moisenz, V. Palichik, V. Perelygin, S. Shmatov, S. Shulha, N. Skatchkov, V. Smirnov, N. Voytishin, A. Zarubin

Petersburg Nuclear Physics Institute, Gatchina (St. Petersburg), Russia
V. Golovtsov, Y. Ivanov, V. Kim[42], E. Kuznetsova[43], P. Levchenko, V. Murzin, V. Oreshkin, I. Smirnov, D. Sosnov, V. Sulimov, L. Uvarov, S. Vavilov, A. Vorobyev

Institute for Nuclear Research, Moscow, Russia
Yu. Andreev, A. Dermenev, S. Gninenko, N. Golubev, A. Karneyeu, M. Kirsanov, N. Krasnikov, A. Pashenkov, A. Shabanov, D. Tlisov, A. Toropin

Institute for Theoretical and Experimental Physics, Moscow, Russia
V. Epshteyn, V. Gavrilov, N. Lychkovskaya, V. Popov, I. Pozdnyakov, G. Safronov, A. Spiridonov, A. Stepennov, V. Stolin, M. Toms, E. Vlasov, A. Zhokin

Moscow Institute of Physics and Technology, Moscow, Russia
T. Aushev

National Research Nuclear University 'Moscow Engineering Physics Institute' (MEPhI), Moscow, Russia
R. Chistov[44], M. Danilov[44], D. Philippov, E. Tarkovskii

P.N. Lebedev Physical Institute, Moscow, Russia
V. Andreev, M. Azarkin, I. Dremin[41], M. Kirakosyan, A. Terkulov

Skobeltsyn Institute of Nuclear Physics, Lomonosov Moscow State University, Moscow, Russia
A. Belyaev, E. Boos, V. Bunichev, M. Dubinin[45], L. Dudko, A. Ershov, V. Klyukhin, O. Kodolova, I. Lokhtin, S. Obraztsov, M. Perfilov, S. Petrushanko, V. Savrin

Novosibirsk State University (NSU), Novosibirsk, Russia
A. Barnyakov[46], V. Blinov[46], T. Dimova[46], L. Kardapoltsev[46], Y. Skovpen[46]

Institute for High Energy Physics of National Research Centre 'Kurchatov Institute', Protvino, Russia
I. Azhgirey, I. Bayshev, S. Bitioukov, V. Kachanov, A. Kalinin, D. Konstantinov, P. Mandrik, V. Petrov, R. Ryutin, S. Slabospitskii, A. Sobol, S. Troshin, N. Tyurin, A. Uzunian, A. Volkov

National Research Tomsk Polytechnic University, Tomsk, Russia
A. Babaev, S. Baidali, V. Okhotnikov

University of Belgrade: Faculty of Physics and VINCA Institute of Nuclear Sciences
P. Adzic[47], P. Cirkovic, D. Devetak, M. Dordevic, P. Milenovic[48], J. Milosevic

Centro de Investigaciones Energéticas Medioambientales y Tecnológicas (CIEMAT), Madrid, Spain
J. Alcaraz Maestre, A. Álvarez Fernández, I. Bachiller, M. Barrio Luna, J.A. Brochero Cifuentes, M. Cerrada, N. Colino, B. De La Cruz, A. Delgado Peris, C. Fernandez Bedoya, J.P. Fernández Ramos, J. Flix, M.C. Fouz, O. Gonzalez Lopez, S. Goy Lopez, J.M. Hernandez, M.I. Josa, D. Moran, A. Pérez-Calero Yzquierdo, J. Puerta Pelayo, I. Redondo, L. Romero, S. Sánchez Navas, M.S. Soares, A. Triossi

Universidad Autónoma de Madrid, Madrid, Spain
C. Albajar, J.F. de Trocóniz

Universidad de Oviedo, Oviedo, Spain
J. Cuevas, C. Erice, J. Fernandez Menendez, S. Folgueras, I. Gonzalez Caballero, J.R. González Fernández, E. Palencia Cortezon, V. Rodríguez Bouza, S. Sanchez Cruz, J.M. Vizan Garcia

Instituto de Física de Cantabria (IFCA), CSIC-Universidad de Cantabria, Santander, Spain
I.J. Cabrillo, A. Calderon, B. Chazin Quero, J. Duarte Campderros, M. Fernandez, P.J. Fernández Manteca, A. García Alonso, J. Garcia-Ferrero, G. Gomez, A. Lopez Virto, J. Marco, C. Martinez Rivero, P. Martinez Ruiz del Arbol, F. Matorras, J. Piedra Gomez, C. Prieels, T. Rodrigo, A. Ruiz-Jimeno, L. Scodellaro, N. Trevisani, I. Vila, R. Vilar Cortabitarte

University of Ruhuna, Department of Physics, Matara, Sri Lanka
N. Wickramage

CERN, European Organization for Nuclear Research, Geneva, Switzerland
D. Abbaneo, B. Akgun, E. Auffray, G. Auzinger, P. Baillon, A.H. Ball, D. Barney, J. Bendavid,

M. Bianco, A. Bocci, C. Botta, E. Brondolin, T. Camporesi, M. Cepeda, G. Cerminara, E. Chapon, Y. Chen, G. Cucciati, D. d'Enterria, A. Dabrowski, N. Daci, V. Daponte, A. David, A. De Roeck, N. Deelen, M. Dobson, M. Dünser, N. Dupont, A. Elliott-Peisert, F. Fallavollita[49], D. Fasanella, G. Franzoni, J. Fulcher, W. Funk, D. Gigi, A. Gilbert, K. Gill, F. Glege, M. Gruchala, M. Guilbaud, D. Gulhan, J. Hegeman, C. Heidegger, Y. Iiyama, V. Innocente, G.M. Innocenti, A. Jafari, P. Janot, O. Karacheban[20], J. Kieseler, A. Kornmayer, M. Krammer[1], C. Lange, P. Lecoq, C. Lourenço, L. Malgeri, M. Mannelli, A. Massironi, F. Meijers, J.A. Merlin, S. Mersi, E. Meschi, F. Moortgat, M. Mulders, J. Ngadiuba, S. Nourbakhsh, S. Orfanelli, L. Orsini, F. Pantaleo[17], L. Pape, E. Perez, M. Peruzzi, A. Petrilli, G. Petrucciani, A. Pfeiffer, M. Pierini, F.M. Pitters, D. Rabady, A. Racz, M. Rovere, H. Sakulin, C. Schäfer, C. Schwick, M. Selvaggi, A. Sharma, P. Silva, P. Sphicas[50], A. Stakia, J. Steggemann, D. Treille, A. Tsirou, A. Vartak, M. Verzetti, W.D. Zeuner

Paul Scherrer Institut, Villigen, Switzerland
L. Caminada[51], K. Deiters, W. Erdmann, R. Horisberger, Q. Ingram, H.C. Kaestli, D. Kotlinski, U. Langenegger, T. Rohe, S.A. Wiederkehr

ETH Zurich - Institute for Particle Physics and Astrophysics (IPA), Zurich, Switzerland
M. Backhaus, L. Bäni, P. Berger, N. Chernyavskaya, G. Dissertori, M. Dittmar, M. Donegà, C. Dorfer, T.A. Gómez Espinosa, C. Grab, D. Hits, T. Klijnsma, W. Lustermann, R.A. Manzoni, M. Marionneau, M.T. Meinhard, F. Micheli, P. Musella, F. Nessi-Tedaldi, F. Pauss, G. Perrin, L. Perrozzi, S. Pigazzini, M. Reichmann, C. Reissel, D. Ruini, D.A. Sanz Becerra, M. Schönenberger, L. Shchutska, V.R. Tavolaro, K. Theofilatos, M.L. Vesterbacka Olsson, R. Wallny, D.H. Zhu

Universität Zürich, Zurich, Switzerland
T.K. Aarrestad, C. Amsler[52], D. Brzhechko, M.F. Canelli, A. De Cosa, R. Del Burgo, S. Donato, C. Galloni, T. Hreus, B. Kilminster, S. Leontsinis, V.M. Mikuni, I. Neutelings, G. Rauco, P. Robmann, D. Salerno, K. Schweiger, C. Seitz, Y. Takahashi, S. Wertz, A. Zucchetta

National Central University, Chung-Li, Taiwan
T.H. Doan, C.M. Kuo, W. Lin, S.S. Yu

National Taiwan University (NTU), Taipei, Taiwan
P. Chang, Y. Chao, K.F. Chen, P.H. Chen, W.-S. Hou, Y.F. Liu, R.-S. Lu, E. Paganis, A. Psallidas, A. Steen

Chulalongkorn University, Faculty of Science, Department of Physics, Bangkok, Thailand
B. Asavapibhop, N. Srimanobhas, N. Suwonjandee

Çukurova University, Physics Department, Science and Art Faculty, Adana, Turkey
A. Bat, F. Boran, S. Damarseckin, Z.S. Demiroglu, F. Dolek, C. Dozen, I. Dumanoglu, E. Eskut, G. Gokbulut, EmineGurpinar Guler[53], Y. Guler, I. Hos[54], C. Isik, E.E. Kangal[55], O. Kara, A. Kayis Topaksu, U. Kiminsu, M. Oglakci, G. Onengut, K. Ozdemir[56], S. Ozturk[57], A. Polatoz, D. Sunar Cerci[58], U.G. Tok, S. Turkcapar, I.S. Zorbakir, C. Zorbilmez

Middle East Technical University, Physics Department, Ankara, Turkey
B. Isildak[59], G. Karapinar[60], M. Yalvac, M. Zeyrek

Bogazici University, Istanbul, Turkey
I.O. Atakisi, E. Gülmez, M. Kaya[61], O. Kaya[62], Ö. Özçelik, S. Ozkorucuklu[63], S. Tekten, E.A. Yetkin[64]

Istanbul Technical University, Istanbul, Turkey
M.N. Agaras, A. Cakir, K. Cankocak, Y. Komurcu, S. Sen[65]

Institute for Scintillation Materials of National Academy of Science of Ukraine, Kharkov, Ukraine
B. Grynyov

National Scientific Center, Kharkov Institute of Physics and Technology, Kharkov, Ukraine
L. Levchuk

University of Bristol, Bristol, United Kingdom
F. Ball, J.J. Brooke, D. Burns, E. Clement, D. Cussans, O. Davignon, H. Flacher, J. Goldstein, G.P. Heath, H.F. Heath, L. Kreczko, D.M. Newbold[66], S. Paramesvaran, B. Penning, T. Sakuma, D. Smith, V.J. Smith, J. Taylor, A. Titterton

Rutherford Appleton Laboratory, Didcot, United Kingdom
K.W. Bell, A. Belyaev[67], C. Brew, R.M. Brown, D. Cieri, D.J.A. Cockerill, J.A. Coughlan, K. Harder, S. Harper, J. Linacre, K. Manolopoulos, E. Olaiya, D. Petyt, T. Reis, T. Schuh, C.H. Shepherd-Themistocleous, A. Thea, I.R. Tomalin, T. Williams, W.J. Womersley

Imperial College, London, United Kingdom
R. Bainbridge, P. Bloch, J. Borg, S. Breeze, O. Buchmuller, A. Bundock, D. Colling, P. Dauncey, G. Davies, M. Della Negra, R. Di Maria, P. Everaerts, G. Hall, G. Iles, T. James, M. Komm, C. Laner, L. Lyons, A.-M. Magnan, S. Malik, A. Martelli, V. Milosevic, J. Nash[68], A. Nikitenko[7], V. Palladino, M. Pesaresi, D.M. Raymond, A. Richards, A. Rose, E. Scott, C. Seez, A. Shtipliyski, G. Singh, M. Stoye, T. Strebler, S. Summers, A. Tapper, K. Uchida, T. Virdee[17], N. Wardle, D. Winterbottom, J. Wright, S.C. Zenz

Brunel University, Uxbridge, United Kingdom
J.E. Cole, P.R. Hobson, A. Khan, P. Kyberd, C.K. Mackay, A. Morton, I.D. Reid, L. Teodorescu, S. Zahid

Baylor University, Waco, USA
K. Call, J. Dittmann, K. Hatakeyama, H. Liu, C. Madrid, B. McMaster, N. Pastika, C. Smith

Catholic University of America, Washington, DC, USA
R. Bartek, A. Dominguez

The University of Alabama, Tuscaloosa, USA
A. Buccilli, O. Charaf, S.I. Cooper, C. Henderson, P. Rumerio, C. West

Boston University, Boston, USA
D. Arcaro, T. Bose, Z. Demiragli, D. Gastler, S. Girgis, D. Pinna, C. Richardson, J. Rohlf, D. Sperka, I. Suarez, L. Sulak, D. Zou

Brown University, Providence, USA
G. Benelli, B. Burkle, X. Coubez, D. Cutts, M. Hadley, J. Hakala, U. Heintz, J.M. Hogan[69], K.H.M. Kwok, E. Laird, G. Landsberg, J. Lee, Z. Mao, M. Narain, S. Sagir[70], R. Syarif, E. Usai, D. Yu

University of California, Davis, Davis, USA
R. Band, C. Brainerd, R. Breedon, D. Burns, M. Calderon De La Barca Sanchez, M. Chertok, J. Conway, R. Conway, P.T. Cox, R. Erbacher, C. Flores, G. Funk, W. Ko, O. Kukral, R. Lander, M. Mulhearn, D. Pellett, J. Pilot, S. Shalhout, M. Shi, D. Stolp, D. Taylor, K. Tos, M. Tripathi, Z. Wang, F. Zhang

University of California, Los Angeles, USA
M. Bachtis, C. Bravo, R. Cousins, A. Dasgupta, A. Florent, J. Hauser, M. Ignatenko, N. Mccoll, S. Regnard, D. Saltzberg, C. Schnaible, V. Valuev

University of California, Riverside, Riverside, USA
E. Bouvier, K. Burt, R. Clare, J.W. Gary, S.M.A. Ghiasi Shirazi, G. Hanson, G. Karapostoli, E. Kennedy, F. Lacroix, O.R. Long, M. Olmedo Negrete, M.I. Paneva, W. Si, L. Wang, H. Wei, S. Wimpenny, B.R. Yates

University of California, San Diego, La Jolla, USA
J.G. Branson, P. Chang, S. Cittolin, M. Derdzinski, R. Gerosa, D. Gilbert, B. Hashemi, A. Holzner, D. Klein, G. Kole, V. Krutelyov, J. Letts, M. Masciovecchio, S. May, D. Olivito, S. Padhi, M. Pieri, V. Sharma, M. Tadel, J. Wood, F. Würthwein, A. Yagil, G. Zevi Della Porta

University of California, Santa Barbara - Department of Physics, Santa Barbara, USA
N. Amin, R. Bhandari, C. Campagnari, M. Citron, V. Dutta, M. Franco Sevilla, L. Gouskos, R. Heller, J. Incandela, H. Mei, A. Ovcharova, H. Qu, J. Richman, D. Stuart, S. Wang, J. Yoo

California Institute of Technology, Pasadena, USA
D. Anderson, A. Bornheim, J.M. Lawhorn, N. Lu, H.B. Newman, T.Q. Nguyen, J. Pata, M. Spiropulu, J.R. Vlimant, R. Wilkinson, S. Xie, Z. Zhang, R.Y. Zhu

Carnegie Mellon University, Pittsburgh, USA
M.B. Andrews, T. Ferguson, T. Mudholkar, M. Paulini, M. Sun, I. Vorobiev, M. Weinberg

University of Colorado Boulder, Boulder, USA
J.P. Cumalat, W.T. Ford, F. Jensen, A. Johnson, E. MacDonald, T. Mulholland, R. Patel, A. Perloff, K. Stenson, K.A. Ulmer, S.R. Wagner

Cornell University, Ithaca, USA
J. Alexander, J. Chaves, Y. Cheng, J. Chu, A. Datta, K. Mcdermott, N. Mirman, J. Monroy, J.R. Patterson, D. Quach, A. Rinkevicius, A. Ryd, L. Skinnari, L. Soffi, S.M. Tan, Z. Tao, J. Thom, J. Tucker, P. Wittich, M. Zientek

Fermi National Accelerator Laboratory, Batavia, USA
S. Abdullin, M. Albrow, M. Alyari, G. Apollinari, A. Apresyan, A. Apyan, S. Banerjee, L.A.T. Bauerdick, A. Beretvas, J. Berryhill, P.C. Bhat, K. Burkett, J.N. Butler, A. Canepa, G.B. Cerati, H.W.K. Cheung, F. Chlebana, M. Cremonesi, J. Duarte, V.D. Elvira, J. Freeman, Z. Gecse, E. Gottschalk, L. Gray, D. Green, S. Grünendahl, O. Gutsche, J. Hanlon, R.M. Harris, S. Hasegawa, J. Hirschauer, Z. Hu, B. Jayatilaka, S. Jindariani, M. Johnson, U. Joshi, B. Klima, M.J. Kortelainen, B. Kreis, S. Lammel, D. Lincoln, R. Lipton, M. Liu, T. Liu, J. Lykken, K. Maeshima, J.M. Marraffino, D. Mason, P. McBride, P. Merkel, S. Mrenna, S. Nahn, V. O'Dell, K. Pedro, C. Pena, O. Prokofyev, G. Rakness, F. Ravera, A. Reinsvold, L. Ristori, A. Savoy-Navarro[71], B. Schneider, E. Sexton-Kennedy, A. Soha, W.J. Spalding, L. Spiegel, S. Stoynev, J. Strait, N. Strobbe, L. Taylor, S. Tkaczyk, N.V. Tran, L. Uplegger, E.W. Vaandering, C. Vernieri, M. Verzocchi, R. Vidal, M. Wang, H.A. Weber

University of Florida, Gainesville, USA
D. Acosta, P. Avery, P. Bortignon, D. Bourilkov, A. Brinkerhoff, L. Cadamuro, A. Carnes, D. Curry, R.D. Field, S.V. Gleyzer, B.M. Joshi, J. Konigsberg, A. Korytov, K.H. Lo, P. Ma, K. Matchev, N. Menendez, G. Mitselmakher, D. Rosenzweig, K. Shi, J. Wang, S. Wang, X. Zuo

Florida International University, Miami, USA
Y.R. Joshi, S. Linn

Florida State University, Tallahassee, USA
A. Ackert, T. Adams, A. Askew, S. Hagopian, V. Hagopian, K.F. Johnson, R. Khurana, T. Kolberg, G. Martinez, T. Perry, H. Prosper, A. Saha, C. Schiber, R. Yohay

Florida Institute of Technology, Melbourne, USA
M.M. Baarmand, V. Bhopatkar, S. Colafranceschi, M. Hohlmann, D. Noonan, M. Rahmani, T. Roy, M. Saunders, F. Yumiceva

University of Illinois at Chicago (UIC), Chicago, USA
M.R. Adams, L. Apanasevich, D. Berry, R.R. Betts, R. Cavanaugh, X. Chen, S. Dittmer, O. Evdokimov, C.E. Gerber, D.A. Hangal, D.J. Hofman, K. Jung, J. Kamin, C. Mills, M.B. Tonjes, N. Varelas, H. Wang, X. Wang, Z. Wu, J. Zhang

The University of Iowa, Iowa City, USA
M. Alhusseini, B. Bilki[53], W. Clarida, K. Dilsiz[72], S. Durgut, R.P. Gandrajula, M. Haytmyradov, V. Khristenko, O.K. Köseyan, J.-P. Merlo, A. Mestvirishvili, A. Moeller, J. Nachtman, H. Ogul[73], Y. Onel, F. Ozok[74], A. Penzo, C. Snyder, E. Tiras, J. Wetzel

Johns Hopkins University, Baltimore, USA
B. Blumenfeld, A. Cocoros, N. Eminizer, D. Fehling, L. Feng, A.V. Gritsan, W.T. Hung, P. Maksimovic, J. Roskes, U. Sarica, M. Swartz, M. Xiao

The University of Kansas, Lawrence, USA
A. Al-bataineh, P. Baringer, A. Bean, S. Boren, J. Bowen, A. Bylinkin, J. Castle, S. Khalil, A. Kropivnitskaya, D. Majumder, W. Mcbrayer, M. Murray, C. Rogan, S. Sanders, E. Schmitz, J.D. Tapia Takaki, Q. Wang

Kansas State University, Manhattan, USA
S. Duric, A. Ivanov, K. Kaadze, D. Kim, Y. Maravin, D.R. Mendis, T. Mitchell, A. Modak, A. Mohammadi

Lawrence Livermore National Laboratory, Livermore, USA
F. Rebassoo, D. Wright

University of Maryland, College Park, USA
A. Baden, O. Baron, A. Belloni, S.C. Eno, Y. Feng, C. Ferraioli, N.J. Hadley, S. Jabeen, G.Y. Jeng, R.G. Kellogg, J. Kunkle, A.C. Mignerey, S. Nabili, F. Ricci-Tam, M. Seidel, Y.H. Shin, A. Skuja, S.C. Tonwar, K. Wong

Massachusetts Institute of Technology, Cambridge, USA
D. Abercrombie, B. Allen, V. Azzolini, A. Baty, R. Bi, S. Brandt, W. Busza, I.A. Cali, M. D'Alfonso, G. Gomez Ceballos, M. Goncharov, P. Harris, D. Hsu, M. Hu, M. Klute, D. Kovalskyi, Y.-J. Lee, P.D. Luckey, B. Maier, A.C. Marini, C. Mcginn, C. Mironov, S. Narayanan, X. Niu, C. Paus, D. Rankin, C. Roland, G. Roland, Z. Shi, G.S.F. Stephans, K. Sumorok, K. Tatar, D. Velicanu, J. Wang, T.W. Wang, B. Wyslouch

University of Minnesota, Minneapolis, USA
A.C. Benvenuti[†], R.M. Chatterjee, A. Evans, P. Hansen, J. Hiltbrand, Sh. Jain, S. Kalafut, M. Krohn, Y. Kubota, Z. Lesko, J. Mans, R. Rusack, M.A. Wadud

University of Mississippi, Oxford, USA
J.G. Acosta, S. Oliveros

University of Nebraska-Lincoln, Lincoln, USA
E. Avdeeva, K. Bloom, D.R. Claes, C. Fangmeier, L. Finco, F. Golf, R. Gonzalez Suarez, R. Kamalieddin, I. Kravchenko, J.E. Siado, G.R. Snow, B. Stieger

State University of New York at Buffalo, Buffalo, USA
A. Godshalk, C. Harrington, I. Iashvili, A. Kharchilava, C. Mclean, D. Nguyen, A. Parker, S. Rappoccio, B. Roozbahani

Northeastern University, Boston, USA
G. Alverson, E. Barberis, C. Freer, Y. Haddad, A. Hortiangtham, G. Madigan, D.M. Morse, T. Orimoto, A. Tishelman-charny, T. Wamorkar, B. Wang, A. Wisecarver, D. Wood

Northwestern University, Evanston, USA
S. Bhattacharya, J. Bueghly, T. Gunter, K.A. Hahn, N. Odell, M.H. Schmitt, K. Sung, M. Trovato, M. Velasco

University of Notre Dame, Notre Dame, USA
R. Bucci, N. Dev, R. Goldouzian, M. Hildreth, K. Hurtado Anampa, C. Jessop, D.J. Karmgard, K. Lannon, W. Li, N. Loukas, N. Marinelli, F. Meng, C. Mueller, Y. Musienko[40], M. Planer, R. Ruchti, P. Siddireddy, G. Smith, S. Taroni, M. Wayne, A. Wightman, M. Wolf, A. Woodard

The Ohio State University, Columbus, USA
J. Alimena, L. Antonelli, B. Bylsma, L.S. Durkin, S. Flowers, B. Francis, C. Hill, W. Ji, A. Lefeld, T.Y. Ling, W. Luo, B.L. Winer

Princeton University, Princeton, USA
S. Cooperstein, G. Dezoort, P. Elmer, J. Hardenbrook, N. Haubrich, S. Higginbotham, A. Kalogeropoulos, S. Kwan, D. Lange, M.T. Lucchini, J. Luo, D. Marlow, K. Mei, I. Ojalvo, J. Olsen, C. Palmer, P. Piroué, J. Salfeld-Nebgen, D. Stickland, C. Tully

University of Puerto Rico, Mayaguez, USA
S. Malik, S. Norberg

Purdue University, West Lafayette, USA
A. Barker, V.E. Barnes, S. Das, L. Gutay, M. Jones, A.W. Jung, A. Khatiwada, B. Mahakud, D.H. Miller, N. Neumeister, C.C. Peng, S. Piperov, H. Qiu, J.F. Schulte, J. Sun, F. Wang, R. Xiao, W. Xie

Purdue University Northwest, Hammond, USA
T. Cheng, J. Dolen, N. Parashar

Rice University, Houston, USA
Z. Chen, K.M. Ecklund, S. Freed, F.J.M. Geurts, M. Kilpatrick, Arun Kumar, W. Li, B.P. Padley, R. Redjimi, J. Roberts, J. Rorie, W. Shi, Z. Tu, A. Zhang

University of Rochester, Rochester, USA
A. Bodek, P. de Barbaro, R. Demina, Y.t. Duh, J.L. Dulemba, C. Fallon, T. Ferbel, M. Galanti, A. Garcia-Bellido, J. Han, O. Hindrichs, A. Khukhunaishvili, E. Ranken, P. Tan, R. Taus

Rutgers, The State University of New Jersey, Piscataway, USA
B. Chiarito, J.P. Chou, Y. Gershtein, E. Halkiadakis, A. Hart, M. Heindl, E. Hughes, S. Kaplan, R. Kunnawalkam Elayavalli, S. Kyriacou, I. Laflotte, A. Lath, R. Montalvo, K. Nash, M. Osherson, H. Saka, S. Salur, S. Schnetzer, D. Sheffield, S. Somalwar, R. Stone, S. Thomas, P. Thomassen

University of Tennessee, Knoxville, USA
H. Acharya, A.G. Delannoy, J. Heideman, G. Riley, S. Spanier

Texas A&M University, College Station, USA
O. Bouhali[75], A. Celik, M. Dalchenko, M. De Mattia, A. Delgado, S. Dildick, R. Eusebi, J. Gilmore, T. Huang, T. Kamon[76], S. Luo, D. Marley, R. Mueller, D. Overton, L. Perniè, D. Rathjens, A. Safonov

Texas Tech University, Lubbock, USA
N. Akchurin, J. Damgov, F. De Guio, P.R. Dudero, S. Kunori, K. Lamichhane, S.W. Lee, T. Mengke, S. Muthumuni, T. Peltola, S. Undleeb, I. Volobouev, Z. Wang, A. Whitbeck

Vanderbilt University, Nashville, USA
S. Greene, A. Gurrola, R. Janjam, W. Johns, C. Maguire, A. Melo, H. Ni, K. Padeken, F. Romeo, P. Sheldon, S. Tuo, J. Velkovska, M. Verweij, Q. Xu

University of Virginia, Charlottesville, USA
M.W. Arenton, P. Barria, B. Cox, R. Hirosky, M. Joyce, A. Ledovskoy, H. Li, C. Neu, Y. Wang, E. Wolfe, F. Xia

Wayne State University, Detroit, USA
R. Harr, P.E. Karchin, N. Poudyal, J. Sturdy, P. Thapa, S. Zaleski

University of Wisconsin - Madison, Madison, WI, USA
J. Buchanan, C. Caillol, D. Carlsmith, S. Dasu, I. De Bruyn, L. Dodd, B. Gomber[77], M. Grothe, M. Herndon, A. Hervé, U. Hussain, P. Klabbers, A. Lanaro, K. Long, R. Loveless, T. Ruggles, A. Savin, V. Sharma, N. Smith, W.H. Smith, N. Woods

†: Deceased
1: Also at Vienna University of Technology, Vienna, Austria
2: Also at IRFU, CEA, Université Paris-Saclay, Gif-sur-Yvette, France
3: Also at Universidade Estadual de Campinas, Campinas, Brazil
4: Also at Federal University of Rio Grande do Sul, Porto Alegre, Brazil
5: Also at Université Libre de Bruxelles, Bruxelles, Belgium
6: Also at University of Chinese Academy of Sciences, Beijing, China
7: Also at Institute for Theoretical and Experimental Physics, Moscow, Russia
8: Also at Joint Institute for Nuclear Research, Dubna, Russia
9: Also at Helwan University, Cairo, Egypt
10: Now at Zewail City of Science and Technology, Zewail, Egypt
11: Also at Suez University, Suez, Egypt
12: Now at British University in Egypt, Cairo, Egypt
13: Also at Fayoum University, El-Fayoum, Egypt
14: Also at Department of Physics, King Abdulaziz University, Jeddah, Saudi Arabia
15: Also at Université de Haute Alsace, Mulhouse, France
16: Also at Skobeltsyn Institute of Nuclear Physics, Lomonosov Moscow State University, Moscow, Russia
17: Also at CERN, European Organization for Nuclear Research, Geneva, Switzerland
18: Also at RWTH Aachen University, III. Physikalisches Institut A, Aachen, Germany
19: Also at University of Hamburg, Hamburg, Germany
20: Also at Brandenburg University of Technology, Cottbus, Germany
21: Also at Institute of Physics, University of Debrecen, Debrecen, Hungary
22: Also at Institute of Nuclear Research ATOMKI, Debrecen, Hungary
23: Also at MTA-ELTE Lendület CMS Particle and Nuclear Physics Group, Eötvös Loránd

University, Budapest, Hungary
24: Also at Indian Institute of Technology Bhubaneswar, Bhubaneswar, India
25: Also at Institute of Physics, Bhubaneswar, India
26: Also at Shoolini University, Solan, India
27: Also at University of Visva-Bharati, Santiniketan, India
28: Also at Isfahan University of Technology, Isfahan, Iran
29: Also at Plasma Physics Research Center, Science and Research Branch, Islamic Azad University, Tehran, Iran
30: Also at ITALIAN NATIONAL AGENCY FOR NEW TECHNOLOGIES, ENERGY AND SUSTAINABLE ECONOMIC DEVELOPMENT, Bologna, Italy
31: Also at CENTRO SICILIANO DI FISICA NUCLEARE E DI STRUTTURA DELLA MATERIA, Catania, Italy
32: Also at Università degli Studi di Siena, Siena, Italy
33: Also at Scuola Normale e Sezione dell'INFN, Pisa, Italy
34: Also at Kyung Hee University, Department of Physics, Seoul, Korea
35: Also at Riga Technical University, Riga, Latvia
36: Also at International Islamic University of Malaysia, Kuala Lumpur, Malaysia
37: Also at Malaysian Nuclear Agency, MOSTI, Kajang, Malaysia
38: Also at Consejo Nacional de Ciencia y Tecnología, Mexico City, Mexico
39: Also at Warsaw University of Technology, Institute of Electronic Systems, Warsaw, Poland
40: Also at Institute for Nuclear Research, Moscow, Russia
41: Now at National Research Nuclear University 'Moscow Engineering Physics Institute' (MEPhI), Moscow, Russia
42: Also at St. Petersburg State Polytechnical University, St. Petersburg, Russia
43: Also at University of Florida, Gainesville, USA
44: Also at P.N. Lebedev Physical Institute, Moscow, Russia
45: Also at California Institute of Technology, Pasadena, USA
46: Also at Budker Institute of Nuclear Physics, Novosibirsk, Russia
47: Also at Faculty of Physics, University of Belgrade, Belgrade, Serbia
48: Also at University of Belgrade, Belgrade, Serbia
49: Also at INFN Sezione di Pavia ^{a}, Università di Pavia ^{b}, Pavia, Italy
50: Also at National and Kapodistrian University of Athens, Athens, Greece
51: Also at Universität Zürich, Zurich, Switzerland
52: Also at Stefan Meyer Institute for Subatomic Physics (SMI), Vienna, Austria
53: Also at Beykent University, Istanbul, Turkey
54: Also at Istanbul Aydin University, Istanbul, Turkey
55: Also at Mersin University, Mersin, Turkey
56: Also at Piri Reis University, Istanbul, Turkey
57: Also at Gaziosmanpasa University, Tokat, Turkey
58: Also at Adiyaman University, Adiyaman, Turkey
59: Also at Ozyegin University, Istanbul, Turkey
60: Also at Izmir Institute of Technology, Izmir, Turkey
61: Also at Marmara University, Istanbul, Turkey
62: Also at Kafkas University, Kars, Turkey
63: Also at Istanbul University, Istanbul, Turkey
64: Also at Istanbul Bilgi University, Istanbul, Turkey
65: Also at Hacettepe University, Ankara, Turkey
66: Also at Rutherford Appleton Laboratory, Didcot, United Kingdom
67: Also at School of Physics and Astronomy, University of Southampton, Southampton,

United Kingdom
68: Also at Monash University, Faculty of Science, Clayton, Australia
69: Also at Bethel University, St. Paul, USA
70: Also at Karamanoğlu Mehmetbey University, Karaman, Turkey
71: Also at Purdue University, West Lafayette, USA
72: Also at Bingol University, Bingol, Turkey
73: Also at Sinop University, Sinop, Turkey
74: Also at Mimar Sinan University, Istanbul, Istanbul, Turkey
75: Also at Texas A&M University at Qatar, Doha, Qatar
76: Also at Kyungpook National University, Daegu, Korea
77: Also at University of Hyderabad, Hyderabad, India